Koizumi S, Fujishita K, Tsuda M, Shigemoto-Mogami Y, Inoue K (2003) Dynamic inhibition of excitatory synaptic transmission by astrocyte-derived ATP in hippocampal cultures. Proc Natl Acad Sci USA 100:11023–11028

Lazarowski ER, Homolya L, Boucher RC, Harden TK (1997) Direct demonstration of mechanically induced release of cellular UTP and its implication for uridine nucleotide receptor activation. J Biol Chem 272:24348–24354

Lazarowski ER, Boucher RC, Harden TK (2000) Constitutive release of ATP and evidence for major contribution of ecto-nucleotide pyrophosphatase and nucleoside diphosphokinase to extracellular nucleotide concentrations. J Biol Chem 275:31061–31068

Lazarowski ER, Boucher RC, Harden TK (2003a) Mechanisms of release of nucleotides and integration of their action as P2X- and P2Y-receptor activating molecules. Mol Pharmacol 64:785–795

Lazarowski ER, Shea DA, Boucher RC, Harden TK (2003b) Release of cellular UDP-glucose as a potential extracellular signaling molecule. Mol Pharmacol 63:1190–1197

Lee WJ, Shin CY, Yoo BK, Ryu JR, Choi EY, Cheong JH, Ryu JH, Ko KH (2003) Induction of matrix metalloproteinase-9 (MMP-9) in lipopolysaccharide-stimulated primary astrocytes is mediated by extracellular signal-regulated protein kinase 1/2 (Erk1/2). Glia 41:15–24

Lee SR, Kim HY, Rogowska J, Zhao BQ, Bhide P, Parent JM, Lo EH (2006) Involvement of matrix metalloproteinase in neuroblast cell migration from the subventricular zone after stroke. J Neurosci 26:3491–3495

Lelongt B, Bengatta S, Delauche M, Lund LR, Werb Z, Ronco PM (2001) Matrix metalloproteinase 9 protects mice from anti-glomerular basement membrane nephritis through its fibrinolytic activity. J Exp Med 193:793–802

Leveque T, Le Pavec G, Boutet A, Tardieu M, Dormont D, Gras G (2004) Differential regulation of gelatinase A and B and TIMP-1 and -2 by TNFalpha and HIV virions in astrocytes. Microbes Infect 6:157–163

Liu K, Wahlberg P, Ny T (1998) Coordinated and cell-specific regulation of membrane type matrix metalloproteinase 1 (MT1-MMP) and its substrate matrix metalloproteinase 2 (MMP-2) by physiological signals during follicular development and ovulation. Endocrinology 139:4735–4738

Lu L, Tonchev AB, Kaplamadzhiev DB, Boneva NB, Mori Y, Sahara S, Ma D, Nakaya MA, Kikuchi M, Yamashima T (2008) Expression of matrix metalloproteinases in the neurogenic niche of the adult monkey hippocampus after ischemia. Hippocampus 18:1074–1084

Marteau F, Le Poul E, Communi D, Communi D, Labouret C, Savi P, Boeynaems JM, Gonzalez NS (2003) Pharmacological characterization of the human P2Y13 receptor. Mol Pharmacol 64:104–112

Moore DJ, Murdock PR, Watson JM, Faull RL, Waldvogel HJ, Szekeres PG, Wilson S, Freeman KB, Emson PC (2003) GPR105, a novel Gi/o-coupled UDP-glucose receptor expressed on brain glia and peripheral immune cells, is regulated by immunologic challenge: possible role in neuroimmune function. Brain Res Mol Brain Res 118:10–23

Mun-Bryce S, Rosenberg GA (1998) Matrix metalloproteinases in cerebrovascular disease. J Cereb Blood Flow Metab 18:1163–1172

Murata Y, Fujiwara N, Seo JH, Yan F, Liu X, Terasaki Y, Luo Y, Arai K, Ji X, Lo EH (2012) Delayed inhibition of c-Jun N-terminal kinase worsens outcomes after focal cerebral ischemia. J Neurosci 32:8112–8115

Nagase H, Woessner JF Jr (1999) Matrix metalloproteinases. J Biol Chem 274:21491–21494

Nedergaard M, Ransom B, Goldman SA (2003) New roles for astrocytes: redefining the functional architecture of the brain. Trends Neurosci 26:523–530

Newman EA (2003) New roles for astrocytes: regulation of synaptic transmission. Trends Neurosci 26:536–542

Noble LJ, Donovan F, Igarashi T, Goussev S, Werb Z (2002) Matrix metalloproteinases limit functional recovery after spinal cord injury by modulation of early vascular events. J Neurosci 22:7526–7535

Reeves TM, Prins ML, Zhu J, Povlishock JT, Phillips LL (2003) Matrix metalloproteinase inhibition alters functional and structural correlates of deafferentation-induced sprouting in the dentate gyrus. J Neurosci 23:10182–10189

Rosenberg GA (1995) Matrix metalloproteinases in brain injury. J Neurotrauma 12:833–842

Rosenberg GA, Estrada EY, Dencoff JE, Stetler-Stevenson WG (1995) Tumor necrosis factor-alpha-induced gelatinase B causes delayed opening of the blood-brain barrier: an expanded therapeutic window. Brain Res 703:151–155

Rosenberg GA, Estrada EY, Dencoff JE (1998) Matrix metalloproteinases and TIMPs are associated with blood–brain barrier opening after reperfusion in rat brain. Stroke 29:2189–2195

Skelton L, Cooper M, Murphy M, Platt A (2003) Human immature monocyte-derived dendritic cells express the G protein-coupled receptor GPR105 (KIAA0001, P2Y14) and increase intracellular calcium in response to its agonist, uridine diphosphoglucose. J Immunol 171:1941–1949

Slezak M, Pfrieger FW (2003) New roles for astrocytes: regulation of CNS synaptogenesis. Trends Neurosci 26:531–535

Takata F, Dohgu S, Matsumoto J, Takahashi H, Machida T, Wakigawa T, Harada E, Miyaji H, Koga M, Nishioku T, Yamauchi A, Kataoka Y (2011) Brain pericytes among cells constituting the blood-brain barrier are highly sensitive to tumor necrosis factor-alpha, releasing matrix metalloproteinase-9 and migrating in vitro. J Neuroinflamm 8:106

Tsai HH, Li H, Fuentealba LC, Molofsky AV, Taveira-Marques R, Zhuang H, Tenney A, Murnen AT, Fancy SP, Merkle F, Kessaris Ns, Alvarez-Buylla A, Richardson WD, Rowitch DH (2012) Regional astrocyte allocation regulates CNS synaptogenesis and repair. Science 337:358–362

Wu CY, Hsieh HL, Jou MJ, Yang CM (2004) Involvement of p42/p44 MAPK, p38 MAPK, JNK and nuclear factor-kappa B in interleukin-1beta-induced matrix metalloproteinase-9 expression in rat brain astrocytes. J Neurochem 90:1477–1488

Yan P, Hu X, Song H, Yin K, Bateman RJ, Cirrito JR, Xiao Q, Hsu FF, Turk JW, Xu J, Hsu CY, Holtzman DM, Lee JM (2006) Matrix metalloproteinase-9 degrades amyloid-beta fibrils in vitro and compact plaques in situ. J Biol Chem 281:24566–24574

Yang Y, Estrada EY, Thompson JF, Liu W, Rosenberg GA (2006) Matrix metalloproteinase-mediated disruption of tight junction proteins in cerebral vessels is reversed by synthetic matrix metalloproteinase inhibitor in focal ischemia in rat. J Cereb Blood Flow Metab 27(4):697–709

Zhao BQ, Wang S, Kim HY, Storrie H, Rosen BR, Mooney DJ, Wang X, Lo EH (2006) Role of matrix metalloproteinases in delayed cortical responses after stroke. Nat Med 12:441–445

The Endocannabinoid Anandamide Inhibits Voltage-Gated Sodium Channels $Na_v1.2$, $Na_v1.6$, $Na_v1.7$, and $Na_v1.8$ in *Xenopus* Oocytes

Dan Okura, MD,* Takafumi Horishita, MD, PhD,* Susumu Ueno, MD, PhD,† Nobuyuki Yanagihara, PhD,‡ Yuka Sudo, PhD,§ Yasuhito Uezono, MD, PhD,‖ and Takeyoshi Sata, MD, PhD*

BACKGROUND: Anandamide is an endocannabinoid that regulates multiple physiological functions by pharmacological actions, in a manner similar to marijuana. Recently, much attention has been paid to the analgesic effect of endocannabinoids in terms of identifying new pharmacotherapies for refractory pain management, but the mechanisms of the analgesic effects of anandamide are still obscure. Voltage-gated sodium channels are believed to play important roles in inflammatory and neuropathic pain. We investigated the effects of anandamide on 4 neuronal sodium channel α subunits, $Na_v1.2$, $Na_v1.6$, $Na_v1.7$, and $Na_v1.8$, to explore the mechanisms underlying the antinociceptive effects of anandamide.

METHODS: We studied the effects of anandamide on $Na_v1.2$, $Na_v1.6$, $Na_v1.7$, and $Na_v1.8$ α subunits with β_1 subunits by using whole-cell, 2-electrode, voltage-clamp techniques in *Xenopus* oocytes.

RESULTS: Anandamide inhibited sodium currents of all subunits at a holding potential causing half-maximal current ($V_{1/2}$) in a concentration-dependent manner. The half-maximal inhibitory concentration values for $Na_v1.2$, $Na_v1.6$, $Na_v1.7$, and $Na_v1.8$ were 17, 12, 27, and 40 μmol/L, respectively, indicating an inhibitory effect on $Na_v1.6$, which showed the highest potency. Anandamide raised the depolarizing shift of the activation curve as well as the hyperpolarizing shift of the inactivation curve in all α subunits, suggesting that sodium current inhibition was due to decreased activation and increased inactivation. Moreover, anandamide showed a use-dependent block in $Na_v1.2$, $Na_v1.6$, and $Na_v1.7$ but not $Na_v1.8$.

CONCLUSION: Anandamide inhibited the function of α subunits in neuronal sodium channels $Na_v1.2$, $Na_v1.6$, $Na_v1.7$, and $Na_v1.8$. These results help clarify the mechanisms of the analgesic effects of anandamide. (Anesth Analg 2014;118:554–62)

Cannabis has been used as a pleasure-inducing drug and traditional medicine for thousands of years, and since the 2 cannabinoid receptors CB_1[1,2] and CB_2[3] were identified, the endocannabinoid signaling system has been a focus of medical research and has been considered a potential therapeutic target.[4] Endocannabinoids mimic the pharmacological actions of the psychoactive principle agent in marijuana, Δ^9-tetrahydrocannabinol, and regulate multiple physiological functions, such as analgesia, regulation of food intake, immunomodulation, inflammation, addictive behavior, epilepsy, and others.[5]

Anandamide, the ethanolamide of arachidonic acid, was the first endocannabinoid isolated from the brain[6]; it acts as a partial agonist on CB_1 receptors, with a lesser effect on CB_2 receptors.[7] Several groups have shown an analgesic effect of exogenous anandamide through the CB_1 receptor in acute,[8–10] persistent inflammatory,[11–13] and neuropathic pain models.[14,15] CB_1 receptors are distributed throughout the pain pathways of the central nervous system (CNS), including the periaqueductal gray, amygdala, and spinal trigeminal tract,[16,17] and the peripheral nervous system including the dorsal root ganglion (DRG),[18] suggesting an analgesic effect of anandamide via CB_1 receptors. However, anandamide may also act on other ion channels consisting of pain signaling pathways, including voltage-gated Ca^{2+} channels, TASK1 channels, $5\text{-}HT_3$ receptor, rectifying K^+ channels, and N-methyl-D-aspartate receptors[19–24]; thus, the mechanisms of the analgesic effects of anandamide remain unclear.

Voltage-gated sodium channels play an essential role in action potential initiation and propagation in excitable nerve and muscle cells. Nine distinct pore-forming α subunits ($Na_v1.1$–$Na_v1.9$), which are associated with auxiliary β subunits, have been identified,[25,26] and each has a different pattern of development and localization as well as distinct physiological and pathophysiological roles. Sodium channel α subunits expressed in DRG ($Na_v1.7$, $Na_v1.8$, $Na_v1.9$) are believed to play crucial roles in inflammatory and neuropathic pain and are considered potential targets of these conditions.[27–30] Previous studies have shown that anandamide inhibits sodium channel function in the brain through the inhibition of veratridine-dependent depolarization of synaptosomes[31] and suppresses tetrodotoxin-sensitive (TTX-S) and tetrodotoxin-resistant (TTX-R) sodium currents in rat

From the *Department of Anesthesiology, School of Medicine; †Department of Occupational Toxicology, Institute of Industrial Ecological Sciences, University of Occupational and Environmental Health, ‡Department of Pharmacology, School of Medicine, University of Occupational and Environmental Health, Fukuoka; §Department of Molecular Pathology & Metabolic Disease, Faculty of Pharmaceutical Sciences, Tokyo university of Science, Chiba; and ‖Cancer Pathophysiology Division, National Cancer Center Research Institute, Tokyo, Japan.

Accepted for publication November 15, 2013.

Funding: This study was supported by a Grant-in-Aid for Scientific Research from the Ministry of Education, Culture, Sports, Science and Technology, 24592369 (to T.H.).

The authors declare no conflicts of interest.

Reprints will not be available from the authors.

Address correspondence to Takafumi Horishita, MD, PhD, Department of Anesthesiology, School of Medicine, University of Occupational and Environmental Health, 1-1 Iseigaoka, Yahatanishiku, Kitakyushu, Fukuoka 807–8555, Japan. Address e-mail to thori@med.uoeh-u.ac.jp.

DOI: 10.1213/ANE.0000000000000070

DRG neurons.[32] These results suggest that sodium channels are potential targets for anandamide. However, the precise mechanisms of anandamide on each α subunit are still unknown. It is of great importance to clarify these mechanisms because each α subunit has a difference of 20% to 50% in amino acid sequence in the transmembrane and extracellular domains and therefore has different physiological functions. Here, we explored the effects of anandamide on several sodium channel α subunits, including $Na_v1.2$, that is expressed primarily in the CNS; $Na_v1.6$ that is expressed in the CNS and DRG neurons; and $Na_v1.7$ and $Na_v1.8$ that are expressed in DRG neurons.

METHODS

This study was approved by the Animal Research Committee of the University of Occupational and Environmental Health.

Materials

Adult female *Xenopus laevis* frogs were obtained from Kyudo Co., Ltd. (Saga, Japan). Anandamide was purchased from Sigma-Aldrich (St. Louis, MO). Rat $Na_v1.2$ α subunit cDNA was a gift from Dr. W. A. Catterall (University of Washington, Seattle, WA). Rat $Na_v1.6$ α subunit cDNA was a gift from Dr. A. L. Goldin (University of California, Irvine, CA). Rat $Na_v1.7$ α subunit cDNA was a gift from G. Mandel (Oregon Health and Science University, Portland, OR). Rat $Na_v1.8$ α subunit cDNA was a gift from Dr. A. N. Akopian (University of Texas Health Science Center, San Antonio, TX), and human β_1 subunit cDNA was a gift from Dr. A. L. George (Vanderbilt University, Nashville, TN).

cRNA Preparation and Oocyte Injection

After linearization of cDNA with *Cla*I ($Na_v1.2$ α subunit), *Not*I ($Na_v1.6$, 1.7 α subunit), *Xba*I ($Na_v1.8$ α subunit), and *Eco*RI (β_1 subunit), cRNAs were transcribed by using SP6 (1.8 α, β_1 subunit) or T7 ($Na_v1.2$, 1.6 1.7 α subunit) RNA polymerase from the mMESSAGE mMACHINE kit (Ambion, Austin, TX). Preparation of *X. laevis* oocytes and cRNA microinjection were performed as described previously.[33] Briefly, stage IV to VI oocytes were manually isolated from a removed portion of ovary. Next, oocytes were treated with collagenase (0.5 mg/mL) for 10 minutes and placed in modified Barth's solution (88 mmol/L NaCl, 1 mmol/L KCl, 2.4 mmol/L $NaHCO_3$, 10 mmol/L HEPES, 0.82 mmol/L $MgSO_4$, 0.33 mmol/L $Ca(NO_3)_2$, and 0.91 mmol/L $CaCl_2$, adjusted to pH 7.5), supplemented with 10,000 U penicillin, 50 mg gentamicin, 90 mg theophylline, and 220 mg sodium pyruvate per liter (incubation medium). Na_v α subunit cRNAs were coinjected with β_1 subunit cRNA at a ratio of 1:10 (total volume was 20–40 ng/50 nL) into *Xenopus* oocytes (all α subunits were coinjected with the β_1 subunit). Injected oocytes were incubated at 19°C in incubation medium, and 2 to 6 days after injection, the cells were used for electrophysiological recordings.

Electrophysiological Recordings

All electrical recordings were performed at room temperature (23°C). Oocytes were placed in a 100 μL recording chamber and perfused at 2 mL/min with Frog Ringer's solution containing 115 mmol/L NaCl, 2.5 mmol/L KCl, 10 mmol/L HEPES, 1.8 mmol/L $CaCl_2$, pH 7.2, by using a peristaltic pump (World Precision Instruments Inc., Sarasota, FL). Recording electrodes were prepared with borosilicate glass by using a puller (PP-830, Narishige group company, Tokyo, Japan), and microelectrodes were filled with 3 mol KCl/0.5% low-melting-point agarose with resistances between 0.3 and 0.5 MΩ. The whole-cell voltage clamp was achieved through these 2 electrodes by using a Warner Instruments model OC-725C (Warner, Hamden, CT). Currents were recorded and analyzed by using pCLAMP 7.0 software (Axon Instruments, Foster City, CA), and the amplitude of expressed sodium currents was typically 2 to 15 μA. Transients and leak currents were subtracted by using the P/N procedure. Anandamide stocks were prepared in dimethylsulphoxide (DMSO) and diluted in Frog Ringer's solution to a final DMSO concentration not exceeding 0.05%. Anandamide was then perfused for 5 to 10 minutes to reach equilibrium.

The voltage dependence of activation was determined by using 50-millisecond depolarizing pulses from a holding potential causing maximal current, V_{max} (–90 mV for $Na_v1.2$ and $Na_v1.6$ or –100 mV for $Na_v1.7$ and $Na_v1.8$), and from a holding potential causing half-maximal current, $V_{1/2}$ (from approximately –40 mV to –70 mV) to 50 mV in 10 mV increments. Normalized activation curves were fitted to the Boltzmann equation: $G/G_{max} = 1/(1 + \exp(V_{1/2} - V)/k)$, where G is the voltage-dependent sodium conductance, G_{max} is the maximal sodium conductance, G/G_{max} is the normalized fractional conductance, $V_{1/2}$ is the potential at which activation is half maximal, and k is the slope factor. The G value for each oocyte was calculated by using the formula $G = I/(Vt - Vr)$, where I is the peak sodium current, Vt is the test potential and Vr is the reversal potential. The Vr for each oocyte was estimated by extrapolating the linear ascending segment of the current voltage relationship (I–V) curve to the voltage axis. To measure steady-state inactivation, currents were elicited by a 50-millisecond test pulse to –20 mV for $Na_v1.2$ and $Na_v1.6$ or –10 mV for $Na_v1.7$ or +10 mV for $Na_v1.8$ after 200 milliseconds (500 milliseconds for only $Na_v1.8$) prepulses ranging from –140 mV to 0 mV in 10 mV increments from a holding potential of V_{max}. Steady-state inactivation curves were fitted to the Boltzmann equation: $I/I_{max} = 1/(1 + \exp(V_{1/2} - V)/k)$, where I_{max} is the maximal sodium current, I/I_{max} is the normalized current, $V_{1/2}$ is the voltage of half-maximal inactivation, and k is the slope factor. To investigate a use-dependent sodium channel block of anandamide, currents were elicited at 10 Hz by a 20-millisecond depolarizing pulse of –20 mV for $Na_v1.2$ and $Na_v1.6$ or –10 mV for $Na_v1.7$ or +10 mV for $Na_v1.8$ from a $V_{1/2}$ holding potential in both the absence and presence of 30 μmol/L anandamide. Peak currents were measured and normalized to the first pulse and plotted against the pulse number. Data were fitted to the monoexponential equation $I_{Na} = \exp(-\tau_{use} \cdot n) + C$, where n is pulse number, C is the plateau I_{Na}, and τ_{use} is the time constant of use-dependent decay.

Data Analysis

All values are presented as the mean ± SEM (n = 5–8). The n values refer to the number of oocytes examined. Each experiment was performed with oocytes from at least 2 frogs.

Control sodium current recorded in absence of anandamide was assigned a value of 100%. Data were statistically evaluated by paired *t* test by using GraphPad Prism software (GraphPad Software, Inc., San Diego, CA). Hill slope and half-maximal inhibitory concentration values were also calculated by using this software.

RESULTS

Effects of Anandamide on Peak Na+ Inward Currents

Currents were elicited by using a 50-millisecond depolarizing pulse to –20 mV for $Na_v1.2$ and $Na_v1.6$ or –10 mV for $Na_v1.7$ or +10 mV for $Na_v1.8$ applied every 10 seconds from V_{max} or $V_{1/2}$ holding potential in both the absence and presence of 10 μmol/L anandamide (Fig. 1); anandamide was applied for 10 minutes. Anandamide inhibited the peak I_{Na} induced by all α subunits more potently at $V_{1/2}$ than V_{max}. Anandamide reduced the peak I_{Na} induced by $Na_v1.2$, $Na_v1.6$, $Na_v1.7$, and $Na_v1.8$ by 46 ± 4, 49 ± 3, 37 ± 2, and 27 ± 2 at $V_{1/2}$, respectively, and 7 ± 2, 6 ± 1, 9 ± 1, and 21 ± 5% at V_{max}, respectively (Fig. 2). Inhibition of anandamide at $V_{1/2}$ was statistically significant in all α subunits, but those at V_{max} were not statistically significant except for the suppression in $Na_v1.8$ by paired *t* test. Because suppression at $V_{1/2}$ was potent, we examined the concentration-response relation for anandamide inhibition of the peak I_{Na} induced by $Na_v1.2$, $Na_v1.6$, $Na_v1.7$, and $Na_v1.8$ at $V_{1/2}$ holding potential (Fig. 3). The peak current amplitude in the presence of anandamide was normalized to that in the control, and the effects of anandamide were expressed as percentages of the control. Nonlinear regression analyses of the dose-response curves yielded half-maximal inhibitory concentration values and Hill slopes of 17 ± 3 μmol/L and 0.74 ± 0.04 for $Na_v1.2$, 12 ± 1 μmol/L and 0.79 ± 0.08 for $Na_v1.6$, 27 ± 3 μmol/L and 0.52 ± 0.06 for $Na_v1.7$, 40 ± 14 μmol/L and 0.71 ± 0.10 for $Na_v1.8$, respectively (Fig. 3).

Effects of Anandamide on Sodium Current Activation

We examined the effects of anandamide on 4 α subunits of sodium current activation. Voltage dependence of activation was determined by using 50-millisecond depolarizing pulses from a holding potential of V_{max} to 50 mV in 10 mV increments or from a holding potential of $V_{1/2}$ to 50 mV in 10 mV increments for $Na_v1.2$, $Na_v1.6$, $Na_v1.7$, and $Na_v1.8$. Activation curves were derived from the I-V curves (see Methods); anandamide (30 μmol/L) was applied for 5 minutes. The peak I_{Na} was reduced by anandamide at V_{max} and $V_{1/2}$ holding potentials with all subunits (Fig. 4). Anandamide shifted the midpoint of steady-state activation ($V_{1/2}$) in a depolarizing direction at both holding potentials for all subunits (Fig. 5). These shifts were small (1.9–3.8 mV) but statistically significant (Table 1).

Effects of Anandamide on Sodium Current Inactivation

The effect of anandamide on steady-state inactivation was also investigated. Currents were elicited by a 50-millisecond test pulse to –20 mV for $Na_v1.2$ and $Na_v1.6$ or –10 mV for $Na_v1.7$ or +10 mV for $Na_v1.8$ after 200 millis econds(500 milliseconds for only $Na_v1.8$) prepulses ranging from –140 mV to 0 mV in 10 mV increments from a holding potential of V_{max}. Steady-state inactivation curves were fitted to the Boltzmann equation (see Methods); anandamide (30 μmol/L) was applied for 5 minutes. Anandamide significantly shifted the midpoint of steady-state inactivation ($V_{1/2}$) in the hyperpolarizing direction by 5.2, 5.0, 4.1, and 6.3 mV in $Na_v1.2$, $Na_v1.6$, $Na_v1.7$, and $Na_v1.8$, respectively (Fig. 6, Table 1).

Use-Dependent Block of Sodium Currents by Anandamide

We investigated the use-dependent block of sodium currents by anandamide. Currents were elicited at 10 Hz by a 20-millisecond depolarizing pulse of –20 mV for $Na_v1.2$ and $Na_v1.6$ or –10 mV for $Na_v1.7$ or +10 mV for $Na_v1.8$ from a $V_{1/2}$ holding potential in both the absence and presence of 30 μmol/L anandamide. Peak currents were measured and normalized to the first pulse and plotted against the pulse number (Fig. 7, A–D). Data were fitted by the monoexponential equation (see Methods); anandamide was applied for 5 minutes. Anandamide significantly reduced the plateau I_{Na} amplitude of $Na_v1.2$, $Na_v1.6$, and $Na_v1.7$ from 0.74 ± 0.02 to 0.66 ± 0.03, 0.88 ± 0.01 to 0.66 ± 0.02, and 0.73 ±

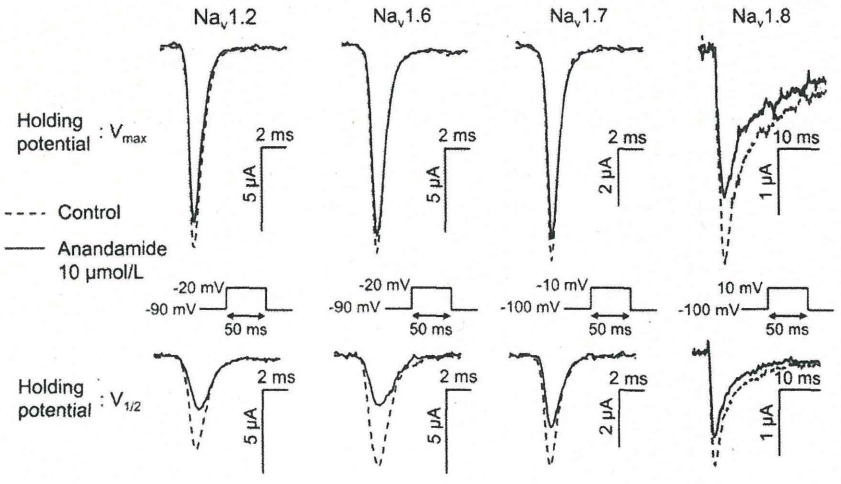

Figure 1. Inhibitory effects of anandamide on peak sodium inward currents in *Xenopus* oocytes expressing $Na_v1.2$, $Na_v1.6$, $Na_v1.7$, and $Na_v1.8$ α subunits with β_1 subunits at 2 holding potentials. Representative traces are shown. Sodium currents were evoked by 50-millisecond depolarizing pulses to –20 mV for $Na_v1.2$ and $Na_v1.6$ or –10 mV for $Na_v1.7$ or +10 mV for $Na_v1.8$ from V_{max} holding potential (upper panel) or $V_{1/2}$ holding potential (lower panel) in both the absence and presence of 10 μmol/L anandamide; anandamide was applied for 10 minutes.

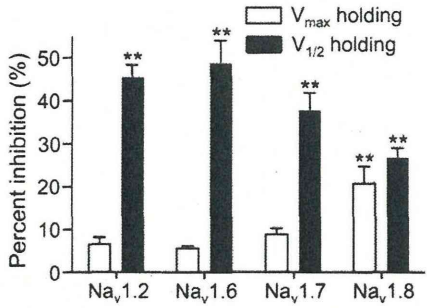

Figure 2. Inhibitory effects of anandamide on peak sodium inward currents in *Xenopus* oocytes expressing $Na_v1.2$, $Na_v1.6$, $Na_v1.7$, and $Na_v1.8$ α subunits with β_1 subunits at 2 holding potentials. Percent inhibition of sodium current of anandamide was calculated. Open columns represent the effect at V_{max} holding potential, and closed columns indicate the effect at $V_{1/2}$ holding potential. Anandamide inhibited the peak I_{Na} induced by $Na_v1.2$, $Na_v1.6$, $Na_v1.7$, and $Na_v1.8$ by 46 ± 4, 49 ± 3, 37 ± 2, and 27 ± 2 at $V_{1/2}$, respectively, and 7 ± 2, 6 ± 1, 9 ± 1, and 21 ± 5% at V_{max}, respectively. Data are represented as the mean ± SEM (n = 5–7). $^{**}P < 0.01$, compared with the control (based on paired t test).

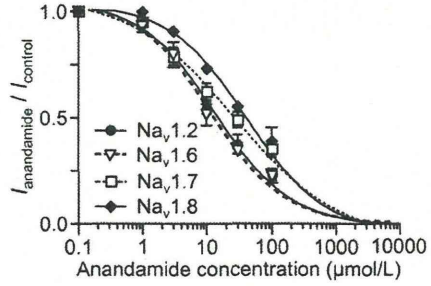

Figure 3. Concentration-response curves for anandamide suppression of sodium currents elicited by 50-millisecond depolarizing pulses to –20 mV for $Na_v1.2$ and $Na_v1.6$ or –10 mV for $Na_v1.7$ or +10 mV for $Na_v1.8$ from $V_{1/2}$ holding potential. The peak current amplitude in the presence of anandamide was normalized to that in the control, and the effects of anandamide are expressed as percentages of the control. Half-maximal inhibitory concentration values and Hill slopes were 17 ± 3 μmol/L and 0.74 ± 0.04 for $Na_v1.2$, 12 ± 1 μmol/L and 0.79 ± 0.08 for $Na_v1.6$, 27 ± 3 μmol/L and 0.52 ± 0.06 for $Na_v1.7$, and 40 ± 14 μmol/L and 0.71 ± 0.10 for $Na_v1.8$, respectively. Data are represented as the mean ± SEM (n = 5–8). Data were fit to the Hill slope equation to give the half-maximal inhibitory concentration values and Hill slopes. Half-maximal inhibitory concentration values and Hill slopes were calculated by using GraphPad Prism.

0.03 to 0.57 ± 0.04, respectively (Fig. 7E), demonstrating a use-dependent block, whereas anandamide did not reduce the plateau I_{Na} amplitude of $Na_v1.8$ (from 0.86 ± 0.03 to 0.84 ± 0.04).

DISCUSSION

In the present study, we demonstrated that anandamide suppresses the $Na_v1.2$, $Na_v1.6$, $Na_v1.7$, and $Na_v1.8$ α subunits in a concentration-dependent manner. half-maximal inhibitory concentration values ranged from 12 μmol/L ($Na_v1.6$) to 40 μmol/L ($Na_v1.8$). Wiley et al.[34] have reported that IV administration of anandamide produce a dose-dependent antinociceptive effect in the tail-flick test with mice, and the 50% effective dose (ED_{50}) of that was 15 mg/kg. They also have shown that the plasma concentration of anandamide was 4.96 μg/mL (14.3 μmol/L) when 10 mg/kg of anandamide was administered, suggesting that half-maximal inhibitory concentration values used in the present study are pharmacologically relevant and are close to the plasma concentration exhibiting an antinociceptive effect by anandamide. We also demonstrated that anandamide has more potent inhibitory effects on sodium currents at $V_{1/2}$ holding potential (inactivated state) than at V_{max} holding potential (resting state) in a manner similar to that of local anesthetics on sodium channels. Therefore, the analgesic effects of anandamide may be mediated through sodium channel blockade. The present results are partially consistent with previous reports that anandamide suppresses TTX-S veratridine-dependent depolarization of synaptosomes, the binding of batrachotoxin to sodium channels, and TTX-S sustained repetitive firing in cortical neurons[31] and inhibits TTX-S and TTX-R sodium currents in a concentration-dependent manner in rat DRG neurons.[32] However, their precise mechanisms of anandamide on several sodium channel α subunits have not yet been investigated. Considering that $Na_v1.6$ was distributed in both CNS and DRG neurons, and that $Na_v1.8$ was distributed in DRG neurons, our results are consistent with a previous study showing that anandamide inhibited sodium currents with half-maximal inhibitory concentration values of 5.4 μmol/L for the TTX-S current and 38 μmol/L for the TTX-R current in DRG neurons,[32] suggesting that TTX-S and TTX-R currents in DRG neurons may represent $Na_v1.6$ and $Na_v1.8$ currents, respectively. Because $Na_v1.6$ is expressed in both the brain and DRG, and anandamide suppressed $Na_v1.6$ function most potently among the 4 α subunits, the effect of anandamide on $Na_v1.6$ may be the most important.

The effects of anandamide on channel gating, including activation and inactivation, demonstrated common characteristics among the 4 α subunits we studied. Anandamide shifted the midpoint of steady-state activation ($V_{1/2}$) in a depolarizing direction at both $V_{1/2}$ and V_{max} holding potentials for all α subunits, and the shifts were significant, although the shifts were small (approximately 4 mV). Anandamide also significantly shifted the midpoint of steady-state inactivation ($V_{1/2}$) in the hyperpolarizing direction (approximately 7 mV) for all α subunits. These results suggest that both inhibition of activation and the enhancement of inactivation are common mechanisms of sodium current inhibition by anandamide for $Na_v1.2$, $Na_v1.6$, $Na_v1.7$, and $Na_v1.8$. A combination of effects on both activation and inactivation might produce sufficient effects to suppress sodium currents although each effect is small. Inhibition by anandamide at V_{max} holding potential for $Na_v1.2$, $Na_v1.6$, and $Na_v1.7$ was small and not significant, whereas that for $Na_v1.8$ was significant (Fig. 1), indicating that resting-channel block is one of the important mechanisms of anandamide inhibition for only $Na_v1.8$. Anandamide exhibited use-dependent block with repetitive stimuli for $Na_v1.2$, $Na_v1.6$, and $Na_v1.7$ but not $Na_v1.8$. The presence of use-dependent block by anandamide suggests the possibility of open-channel block and the ability to slow the recovery time from blocks that are seen with amitriptyline.[35] Sodium channel blockers such as local anesthetics, tricyclic antidepressants, and volatile anesthetics have been shown to shift the voltage dependence of steady-state inactivation with no effect on

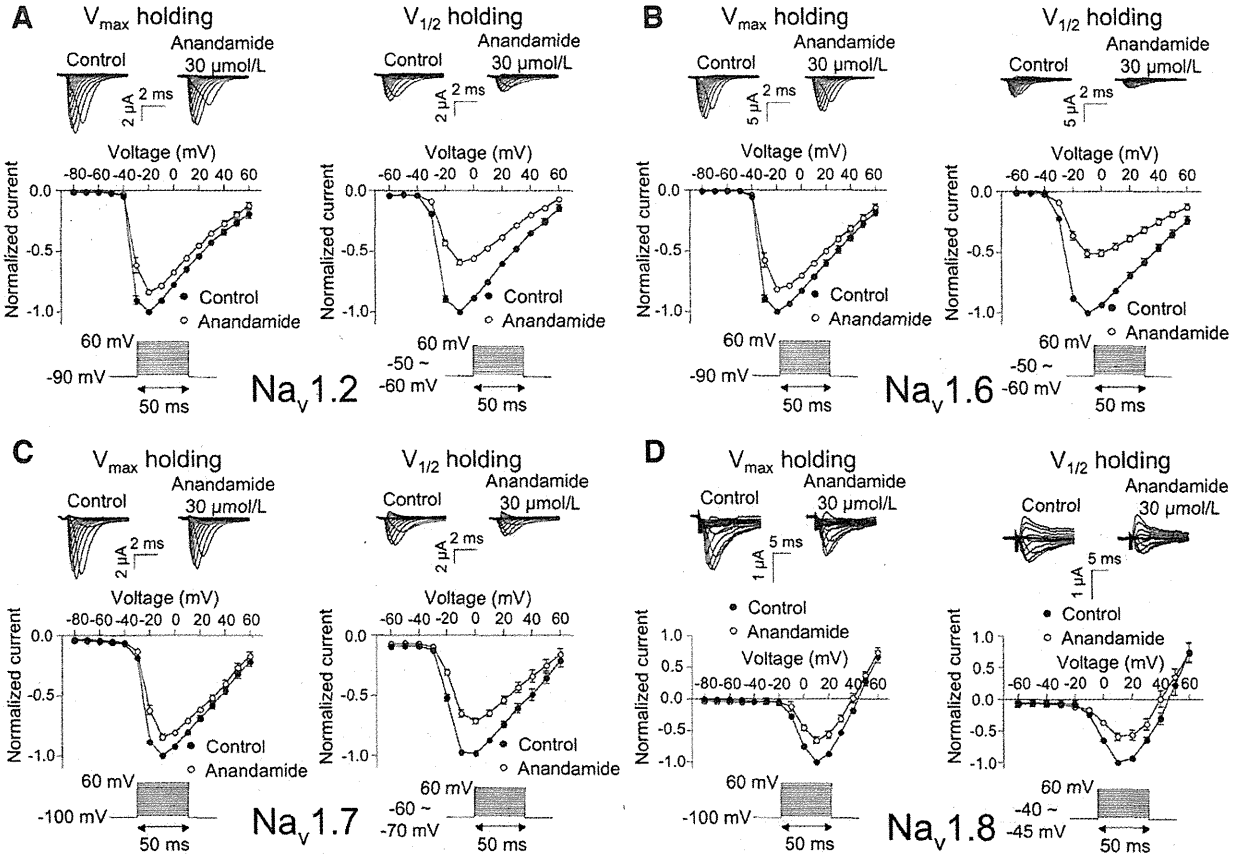

Figure 4. *Effects of anandamide on I-V curves of sodium currents in oocytes expressing* $Na_v1.2$ (A), $Na_v1.6$ (B), $Na_v1.7$ (C), and $Na_v1.8$ (D) α subunits with β_1 subunits. Currents were elicited by using 50-millisecond depolarizing steps between –80 and 60 mV in 10 mV increments from a V_{max} holding potential (left panel) and elicited by using 50-millisecond depolarizing steps between –60 and 60 mV in 10 mV increments from a $V_{1/2}$ holding potential (right panel); anandamide (30 μmol/L) was applied for 5 minutes; upper panel, representative I_{Na} traces from oocytes expressing $Na_v1.2$, $Na_v1.6$, $Na_v1.7$, and $Na_v1.8$ with β_1 subunits in both the absence and presence of 30 μmol/L anandamide; lower panel, effects of anandamide on representative I-V curves elicited from V_{max} holding potential (left panel) and $V_{1/2}$ holding potential (right panel) (closed circles, control; open circles, anandamide). Peak currents were normalized to the maximal currents observed from –20 to +10 mV. Data are represented as the mean ± SEM (n = 5–8).

activation and exhibit use-dependent block.[35–39] Our results show that anandamide shows a negative shift in the voltage dependence of inactivation and use-dependent block except for $Na_v1.8$ that are seen with other sodium channel blockers yet also shifts the steady-state activation in a depolarizing direction, suggesting that it may have different binding sites or allosteric conformational mechanisms for these sodium channel antagonists. Moreover, a resting-channel block, not an open-channel block, for $Na_v1.8$ may be a key for exploring the mechanism of sodium channel inhibition by anandamide in detail.

Several groups have evaluated antinociception by exogenous anandamide via CB_1 receptors.[8–10] Indeed, a recent review has shown that activation of both CB_1 and CB_2 receptors reduces nociceptive processing in acute and chronic animal models of pain.[40] Alternatively, other investigators have suggested that anandamide produces antinociception through a CB_1-independent mechanism. For example, anandamide antinociception is not blocked by pretreatment with the selective CB_1 antagonist SR141716A.[41] Rapid metabolism of anandamide to arachidonic acid has been shown to be one of the reasons for the failure of SR141716A to antagonize the effects of anandamide; in experiments, the ability of SR141716A to reverse anandamide antinociception was improved (but not completely) when anandamide metabolism to arachidonic acid was inhibited with coadministration of an amidase inhibitor, phenylmethylsulfonyl fluoride.[42] That study also demonstrated that cyclooxygenase did not alter the effects of anandamide, whereas it blocked the effects of arachidonic acid, suggesting a pain-inhibitory effect of anandamide by noncannabinoid mechanisms. Another recent study suggested that anandamide induced antinociception by stimulating endogenous norepinephrine release that activated peripheral adrenoceptors inducing antinociception, although whether the effect was caused through cannabinoid receptors remains unknown.[43]

This study indicates that sodium channel inhibition by anandamide is independent of signaling through cannabinoid receptors, because in recombinant experiments such as our present examination, the effects on channels or receptors can be excluded except for that expressed in membranes. Previous reports also indicate a direct effect of anandamide on sodium channels by demonstrating that sodium channel-related activities by anandamide in the brain may be independent of

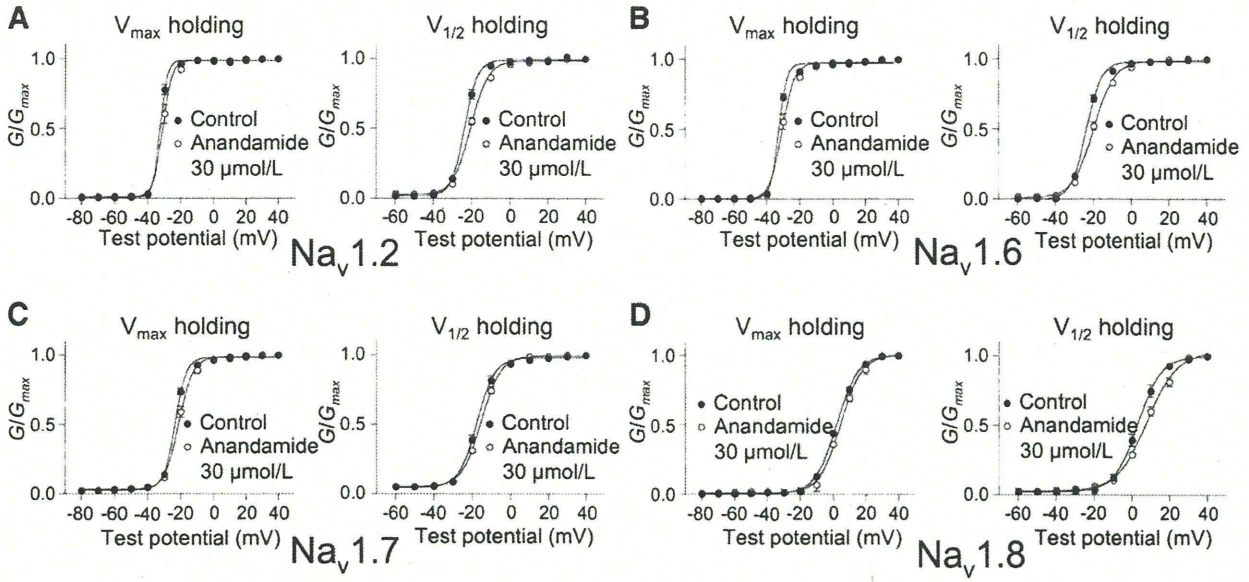

Figure 5. Effects of anandamide on channel activation in oocytes expressing $Na_v1.2$ (A), $Na_v1.6$ (B), $Na_v1.7$ (C), and $Na_v1.8$ (D) α subunits with β_1 subunits from V_{max} holding potential (left panels) or $V_{1/2}$ holding potential (right panels). Closed circles represent control; open circles indicate the effect of anandamide. Data are expressed as the mean ± SEM (n = 5–8). Activation curves were fitted to the Boltzmann equation; $V_{1/2}$ is shown in Table 1.

Table 1. Effects of Anandamide on Activation and Inactivation in Oocytes Expressing $Na_v1.2$, $Na_v1.6$, $Na_v1.7$, and $Na_v1.8$ α Subunits with β_1 Subunits

	$V_{1/2}$ (mV)					
	Holding V_{max}			Holding $V_{1/2}$		
	Control	Anandamide	Shift	Control	Anandamide	Shift
Activation						
$Na_v1.2$	−32.7 ± 0.3	−30.8 ± 0.7*	+1.9	−23.6 ± 0.6	−20.4 ± 0.6**	+3.2
$Na_v1.6$	−32.6 ± 0.3	−30.5 ± 0.7*	+2.1	−23.8 ± 0.5	−20.0 ± 0.6**	+3.8
$Na_v1.7$	−23.4 ± 0.4	−21.0 ± 0.8*	+2.4	−17.3 ± 0.7	−15.0 ± 0.7*	+2.3
$Na_v1.8$	2.2 ± 0.2	4.8 ± 0.8*	+2.6	3.3 ± 1.0	8.4 ± 1.1*	+3.3
Inactivation						
$Na_v1.2$	−51.4 ± 0.7	−56.6 ± 0.8**	−5.2			
$Na_v1.6$	−53.5 ± 0.8	−58.5 ± 1.0**	−5.0			
$Na_v1.7$	−64.3 ± 0.7	−68.4 ± 0.6**	−4.1			
$Na_v1.8$	−50.7 ± 1.4	−57.0 ± 1.9*	−6.3			

*P < 0.05.
**P < 0.01, compared with control (paired t test) (mean ± SEM; n = 5–7).

the presence of AM 251 (a CB_1 antagonist),[31] AM 251, AM 630 (a CB_2 antagonist) and capsazepine (a vanilloid receptor type 1 antagonist) do not interfere with anandamide suppression of sodium currents in DRG.[32] Therefore, we believe that the effects of anandamide on $Na_v1.2$, $Na_v1.6$, $Na_v1.7$, and $Na_v1.8$ α subunits are direct. Taken together, to the best of our knowledge, this is the first direct evidence to demonstrate the inhibitory effects and its mechanisms on neuronal sodium channel α subunits in recombinant experiment systems.

Several sodium channel α subunits are believed to be involved in the pathogenesis of inflammatory and neuropathic pain. Mutations in $Na_v1.7$ have been linked to inherited pain syndromes, including inherited erythromelalgia, that is characterized by episodes of burning pain, erythema, mild swelling in the hands and feet,[44] and paroxysmal extreme pain disorder (PEPD), which is characterized by severe rectal, ocular, and mandibular pain.[45] Recently, anandamide has been reported to inhibit resurgent current of wild-type $Na_v1.7$ and the PEPD mutants expressed in transfected human embryonic kidney 293 cells, and this inhibition was suggested as a therapeutic target for PEPD patients.[46] $Na_v1.8$ has demonstrated its ability to carry most current underlying the upstroke of the action potential in nociceptive neurons,[47] and the use of $Na_v1.8$ knockdown rats after antisense oligodeoxynucleotide treatment has demonstrated a role for $Na_v1.8$ in inflammatory pain,[48] whereas $Na_v1.8$ expression has been reported to increase in nerves proximal to injury sites in patients with chronic neuropathic pain.[49] In an infraorbital nerve injury model of rats, the level of $Na_v1.6$ protein was significantly increased proximal to the lesion site, suggesting a role of $Na_v1.6$ in neuropathic pain conditions.[50] However, these α subunits highly expressed in normal DRG have been reported to show diverse expression in DRG of inflammatory and neuropathic pain models. $Na_v1.7$ mRNA and protein increased in DRG after peripheral inflammation induced by

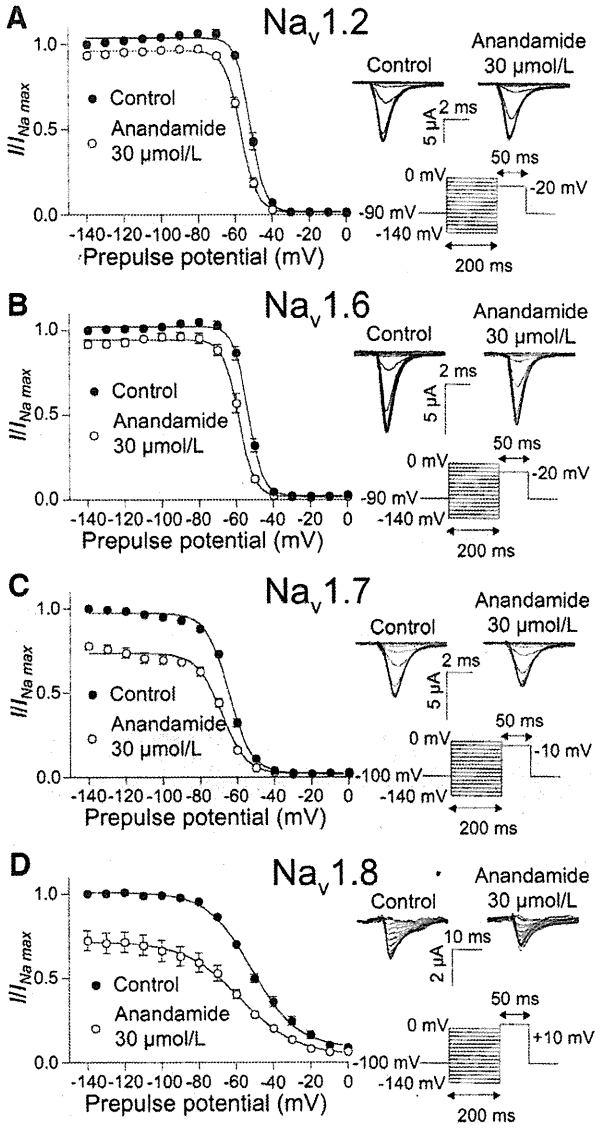

Figure 6. Effects of anandamide on inactivation curves in oocytes expressing $Na_v1.2$ (A), $Na_v1.6$ (B), $Na_v1.7$ (C), and $Na_v1.8$ (D) α subunits with β_1 subunits. Currents were elicited by a 50-millisecond test pulse to –20 mV for $Na_v1.2$ and $Na_v1.6$ or –10 mV for $Na_v1.7$ or +10 mV for $Na_v1.8$ after 200-millisecond (500-millisecond for only $Na_v1.8$) prepulses ranging from –140 mV to 0 mV in 10 mV increments from a holding potential of V_{max}; anandamide (30 μmol/L) was applied for 5 minutes; right panel, representative I_{Na} traces in both the absence and presence of anandamide; left panel, effects of anandamide on inactivation curves (closed circles, control; open circles, anandamide). Steady-state inactivation curves were fitted to the Boltzmann equation, and the $V_{1/2}$ values are shown in Table 1. Data are expressed as the mean ± SEM (n = 6–8).

carrageenan,[51,52] whereas $Na_v1.7$ protein decreased in the injured DRG after spared nerve injury in animals.[53] $Na_v1.8$ mRNA and protein increased in DRG neurons of rodents after injection of carrageenan into a hindpaw,[51,54,55] and yet peripheral nerve injury down-regulates $Na_v1.8$ mRNA and protein expression in the injured DRG.[29,53,56] Based on this evidence, suppression of sensory neuron sodium channel function by anandamide may be an important mechanism independent of the cannabinoid receptor. Because of the

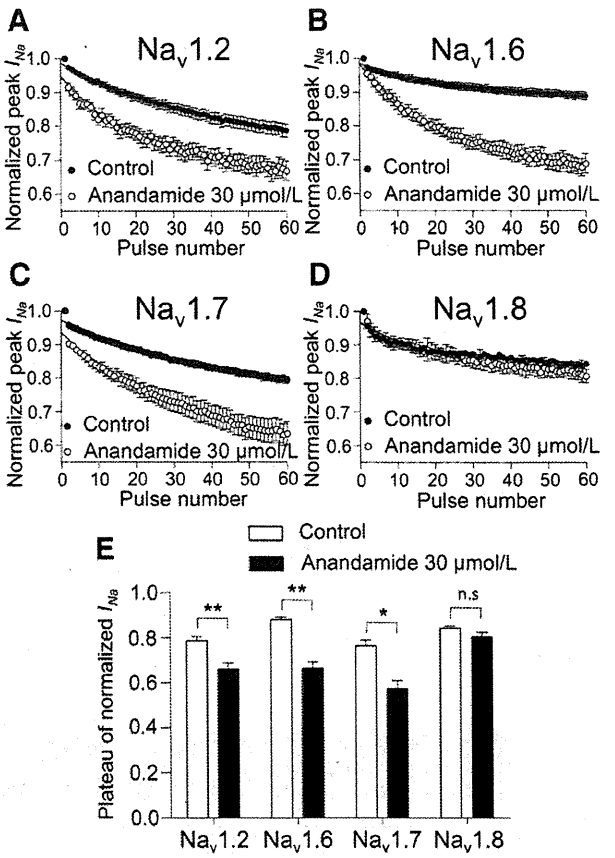

Figure 7. Use-dependent block of sodium channel on $Na_v1.2$, $Na_v1.6$, $Na_v1.7$, and $Na_v1.8$ α subunits with β_1 subunits of anandamide. Currents were elicited at 10 Hz by a 20-millisecond depolarizing pulse of –20 mV for $Na_v1.2$ and $Na_v1.6$, or –10 mV for $Na_v1.7$, or +10 mV for $Na_v1.8$ from a $V_{1/2}$ holding potential in both the absence and presence of 30 μmol/L anandamide; anandamide was applied for 5 minutes. Peak currents were measured and normalized to the first pulse and plotted against the pulse number (A, $Na_v1.2$; B, $Na_v1.6$; C, $Na_v1.7$; D, $Na_v1.8$). Closed circles represent control; open circles indicate the effect of anandamide. Data were fitted to the monoexponential equation, and values for fractional block of the plateau of normalized I_{Na} are shown in (E). Data are expressed as the mean ± SEM (n = 5–6). $^*P < 0.05$ and $^{**}P < 0.01$, compared with the control (paired t test).

limitations of our experiments, further investigation is warranted to extrapolate our findings into clinical practice.

In conclusion, anandamide at pharmacologically relevant concentrations inhibited sodium currents of $Na_v1.2$, $Na_v1.6$, $Na_v1.7$, and $Na_v1.8$ α subunits expressed in the *Xenopus* oocytes with differences in the effects on sodium channel gating. These results provide a better understanding of the mechanisms underlying the analgesic effects of anandamide, but further studies are needed to clarify the relevance of sodium channel inhibition by anandamide to analgesia.

DISCLOSURES

Name: Dan Okura, MD.

Contribution: This author helped data collection, data analysis, and manuscript preparation.

Attestation: Dan Okura approved the final manuscript and attests to the integrity of the original data and the analysis reported in this manuscript.

Name: Takafumi Horishita, MD, PhD.
Contribution: This author helped study design, data collection, data analysis, and manuscript preparation.
Attestation: Takafumi Horishita approved the final manuscript and attests to the integrity of the original data and the analysis reported in this manuscript, and also is the archival author.
Name: Susumu Ueno, MD, PhD.
Contribution: This author helped conduct of the study and manuscript preparation.
Attestation: Susumu Ueno approved the final manuscript.
Name: Nobuyuki Yanagihara, PhD.
Contribution: This author helped conduct of the study and manuscript preparation.
Attestation: Nobuyuki Yanagihara approved the final manuscript.
Name: Yuka Sudo, PhD.
Contribution: This author helped conduct of the study.
Attestation: Yuka Sudo approved the final manuscript.
Name: Yasuhito Uezono, MD, PhD.
Contribution: This author helped conduct of the study.
Attestation: Yasuhito Uezono approved the final manuscript.
Name: Takeyoshi Sata, MD, PhD.
Contribution: This author helped conduct of the study and manuscript preparation.
Attestation: Takeyoshi Sata approved the final manuscript.
This manuscript was handled by: Marcel E. Durieux, MD, PhD.

REFERENCES

1. Devane WA, Dysarz FA 3rd, Johnson MR, Melvin LS, Howlett AC. Determination and characterization of a cannabinoid receptor in rat brain. Mol Pharmacol 1988;34:605–13
2. Matsuda LA, Lolait SJ, Brownstein MJ, Young AC, Bonner TI. Structure of a cannabinoid receptor and functional expression of the cloned cDNA. Nature 1990;346:561–4
3. Munro S, Thomas KL, Abu-Shaar M. Molecular characterization of a peripheral receptor for cannabinoids. Nature 1993;365:61–5
4. Zias J, Stark H, Sellgman J, Levy R, Werker E, Breuer A, Mechoulam R. Early medical use of cannabis. Nature 1993;363:215
5. Pacher P, Bátkai S, Kunos G. The endocannabinoid system as an emerging target of pharmacotherapy. Pharmacol Rev 2006;58:389–462
6. Devane WA, Hanus L, Breuer A, Pertwee RG, Stevenson LA, Griffin G, Gibson D, Mandelbaum A, Etinger A, Mechoulam R. Isolation and structure of a brain constituent that binds to the cannabinoid receptor. Science 1992;258:1946–9
7. Pertwee RG, Ross RA. Cannabinoid receptors and their ligands. Prostaglandins Leukot Essent Fatty Acids 2002;66:101–21
8. Costa B, Vailati S, Colleoni M. SR 141716A, a cannabinoid receptor antagonist, reverses the behavioural effects of anandamide-treated rats. Behav Pharmacol 1999;10:327–31
9. Mason DJ Jr, Lowe J, Welch SP. Cannabinoid modulation of dynorphin A: correlation to cannabinoid-induced antinociception. Eur J Pharmacol 1999;378:237–48
10. Welch SP, Huffman JW, Lowe J. Differential blockade of the antinociceptive effects of centrally administered cannabinoids by SR141716A. J Pharmacol Exp Ther 1998;286:1301–8
11. Calignano A, La Rana G, Giuffrida A, Piomelli D. Control of pain initiation by endogenous cannabinoids. Nature 1998;394:277–81
12. Richardson JD, Kilo S, Hargreaves KM. Cannabinoids reduce hyperalgesia and inflammation via interaction with peripheral CB1 receptors. Pain 1998;75:111–9
13. Guindon J, De Léan A, Beaulieu P. Local interactions between anandamide, an endocannabinoid, and ibuprofen, a nonsteroidal anti-inflammatory drug, in acute and inflammatory pain. Pain 2006;121:85–93
14. Sagar DR, Kendall DA, Chapman V. Inhibition of fatty acid amide hydrolase produces PPAR-alpha-mediated analgesia in a rat model of inflammatory pain. Br J Pharmacol 2008;155:1297–306
15. Karbarz MJ, Luo L, Chang L, Tham CS, Palmer JA, Wilson SJ, Wennerholm ML, Brown SM, Scott BP, Apodaca RL, Keith JM, Wu J, Breitenbucher JG, Chaplan SR, Webb M. Biochemical and biological properties of 4-(3-phenyl-[1,2,4] thiadiazol-5-yl)-piperazine-1-carboxylic acid phenylamide, a mechanism-based inhibitor of fatty acid amide hydrolase. Anesth Analg 2009;108:316–29
16. Tsou K, Brown S, Sañudo-Peña MC, Mackie K, Walker JM. Immunohistochemical distribution of cannabinoid CB1 receptors in the rat central nervous system. Neuroscience 1998;83:393–411
17. Farquhar-Smith WP, Egertová M, Bradbury EJ, McMahon SB, Rice AS, Elphick MR. Cannabinoid CB(1) receptor expression in rat spinal cord. Mol Cell Neurosci 2000;15:510–21
18. Hohmann AG, Herkenham M. Localization of central cannabinoid CB1 receptor messenger RNA in neuronal subpopulations of rat dorsal root ganglia: a double-label in situ hybridization study. Neuroscience 1999;90:923–31
19. Chemin J, Monteil A, Perez-Reyes E, Nargeot J, Lory P. Direct inhibition of T-type calcium channels by the endogenous cannabinoid anandamide. EMBO J 2001;20:7033–40
20. Mackie K, Lai Y, Westenbroek R, Mitchell R. Cannabinoids activate an inwardly rectifying potassium conductance and inhibit Q-type calcium currents in AtT20 cells transfected with rat brain cannabinoid receptor. J Neurosci 1995;15:6552–61
21. Maingret F, Patel AJ, Lazdunski M, Honoré E. The endocannabinoid anandamide is a direct and selective blocker of the background K(+) channel TASK-1. EMBO J 2001;20:47–54
22. Fan P. Cannabinoid agonists inhibit the activation of 5-HT3 receptors in rat nodose ganglion neurons. J Neurophysiol 1995;73:907–10
23. Poling JS, Rogawski MA, Salem N Jr, Vicini S. Anandamide, an endogenous cannabinoid, inhibits Shaker-related voltage-gated K+ channels. Neuropharmacology 1996;35:983–91
24. Mendiguren A, Pineda J. Cannabinoids enhance N-methyl-D-aspartate-induced excitation of locus coeruleus neurons by CB1 receptors in rat brain slices. Neurosci Lett 2004;363:1–5
25. Catterall WA. From ionic currents to molecular mechanisms: the structure and function of voltage-gated sodium channels. Neuron 2000;26:13–25
26. Catterall WA, Goldin AL, Waxman SG. International Union of Pharmacology. XLVII. Nomenclature and structure-function relationships of voltage-gated sodium channels. Pharmacol Rev 2005;57:397–409
27. Wood JN, Boorman JP, Okuse K, Baker MD. Voltage-gated sodium channels and pain pathways. J Neurobiol 2004;61:55–71
28. Cummins TR, Sheets PL, Waxman SG. The roles of sodium channels in nociception: implications for mechanisms of pain. Pain 2007;131:243–57
29. Decosterd I, Ji RR, Abdi S, Tate S, Woolf CJ. The pattern of expression of the voltage-gated sodium channels Na(v)1.8 and Na(v)1.9 does not change in uninjured primary sensory neurons in experimental neuropathic pain models. Pain 2002;96:269–77
30. Wang W, Gu J, Li YQ, Tao YX. Are voltage-gated sodium channels on the dorsal root ganglion involved in the development of neuropathic pain? Mol Pain 2011;7:16
31. Nicholson RA, Liao C, Zheng J, David LS, Coyne L, Errington AC, Singh G, Lees G. Sodium channel inhibition by anandamide and synthetic cannabimimetics in brain. Brain Res 2003;978:194–204
32. Kim HI, Kim TH, Shin YK, Lee CS, Park M, Song JH. Anandamide suppression of Na+ currents in rat dorsal root ganglion neurons. Brain Res 2005;1062:39–47
33. Horishita T, Eger EI 2nd, Harris RA. The effects of volatile aromatic anesthetics on voltage-gated Na+ channels expressed in Xenopus oocytes. Anesth Analg 2008;107:1579–86
34. Wiley JL, Dewey MA, Jefferson RG, Winckler RL, Bridgen DT, Willoughby KA, Martin BR. Influence of phenylmethylsulfonyl fluoride on anandamide brain levels and pharmacological effects. Life Sci 2000;67:1573–83

35. Wang GK, Russell C, Wang SY. State-dependent block of voltage-gated Na+ channels by amitriptyline via the local anesthetic receptor and its implication for neuropathic pain. Pain 2004;110:166–74
36. Ragsdale DS, McPhee JC, Scheuer T, Catterall WA. Molecular determinants of state-dependent block of Na+ channels by local anesthetics. Science 1994;265:1724–8
37. Osawa Y, Oda A, Iida H, Tanahashi S, Dohi S. The effects of class Ic antiarrhythmics on tetrodotoxin-resistant Na+ currents in rat sensory neurons. Anesth Analg 2004;99:464–71, table of contents
38. Poyraz D, Bräu ME, Wotka F, Puhlmann B, Scholz AM, Hempelmann G, Kox WJ, Spies CD. Lidocaine and octanol have different modes of action at tetrodotoxin-resistant Na(+) channels of peripheral nerves. Anesth Analg 2003;97:1317–24
39. Ouyang W, Herold KF, Hemmings HC Jr. Comparative effects of halogenated inhaled anesthetics on voltage-gated Na+ channel function. Anesthesiology 2009;110:582–90
40. Starowicz K, Malek N, Przewlocka B. Cannabinoid receptors and pain. Wiley Interdiscip Rev Membr Transp Signal 2013;2:121–32
41. Adams IB, Compton DR, Martin BR. Assessment of anandamide interaction with the cannabinoid brain receptor: SR 141716A antagonism studies in mice and autoradiographic analysis of receptor binding in rat brain. J Pharmacol Exp Ther 1998;284:1209–17
42. Wiley JL, Razdan RK, Martin BR. Evaluation of the role of the arachidonic acid cascade in anandamide's *in vivo* effects in mice. Life Sci 2006;80:24–35
43. Romero TR, Resende LC, Guzzo LS, Duarte ID. CB1 and CB2 cannabinoid receptor agonists induce peripheral antinociception by activation of the endogenous noradrenergic system. Anesth Analg 2013;116:463–72
44. Waxman SG, Dib-Hajj S. Erythermalgia: molecular basis for an inherited pain syndrome. Trends Mol Med 2005;11:555–62
45. Fertleman CR, Ferrie CD, Aicardi J, Bednarek NA, Eeg-Olofsson O, Elmslie FV, Griesemer DA, Goutières F, Kirkpatrick M, Malmros IN, Pollitzer M, Rossiter M, Roulet-Perez E, Schubert R, Smith VV, Testard H, Wong V, Stephenson JB. Paroxysmal extreme pain disorder (previously familial rectal pain syndrome). Neurology 2007;69:586–95
46. Theile JW, Cummins TR. Inhibition of Navβ4 peptide-mediated resurgent sodium currents in Nav1.7 channels by carbamazepine, riluzole, and anandamide. Mol Pharmacol 2011;80:724–34
47. Renganathan M, Cummins TR, Waxman SG. Contribution of Na(v)1.8 sodium channels to action potential electrogenesis in DRG neurons. J Neurophysiol 2001;86:629–40
48. Joshi SK, Mikusa JP, Hernandez G, Baker S, Shieh CC, Neelands T, Zhang XF, Niforatos W, Kage K, Han P, Krafte D, Faltynek C, Sullivan JP, Jarvis MF, Honore P. Involvement of the TTX-resistant sodium channel Nav 1.8 in inflammatory and neuropathic, but not post-operative, pain states. Pain 2006;123:75–82
49. Black JA, Nikolajsen L, Kroner K, Jensen TS, Waxman SG. Multiple sodium channel isoforms and mitogen-activated protein kinases are present in painful human neuromas. Ann Neurol 2008;64:644–53
50. Henry MA, Freking AR, Johnson LR, Levinson SR. Sodium channel Nav1.6 accumulates at the site of infraorbital nerve injury. BMC Neurosci 2007;8:56
51. Black JA, Liu S, Tanaka M, Cummins TR, Waxman SG. Changes in the expression of tetrodotoxin-sensitive sodium channels within dorsal root ganglia neurons in inflammatory pain. Pain 2004;108:237–47
52. Strickland IT, Martindale JC, Woodhams PL, Reeve AJ, Chessell IP, McQueen DS. Changes in the expression of NaV1.7, NaV1.8 and NaV1.9 in a distinct population of dorsal root ganglia innervating the rat knee joint in a model of chronic inflammatory joint pain. Eur J Pain 2008;12:564–72
53. Berta T, Poirot O, Pertin M, Ji RR, Kellenberger S, Decosterd I. Transcriptional and functional profiles of voltage-gated Na(+) channels in injured and non-injured DRG neurons in the SNI model of neuropathic pain. Mol Cell Neurosci 2008;37:196–208
54. Okuse K, Chaplan SR, McMahon SB, Luo ZD, Calcutt NA, Scott BP, Akopian AN, Wood JN. Regulation of expression of the sensory neuron-specific sodium channel SNS in inflammatory and neuropathic pain. Mol Cell Neurosci 1997;10:196–207
55. Coggeshall RE, Tate S, Carlton SM. Differential expression of tetrodotoxin-resistant sodium channels Nav1.8 and Nav1.9 in normal and inflamed rats. Neurosci Lett 2004;355:45–8
56. Cummins TR, Waxman SG. Downregulation of tetrodotoxin-resistant sodium currents and upregulation of a rapidly repriming tetrodotoxin-sensitive sodium current in small spinal sensory neurons after nerve injury. J Neurosci 1997;17:3503–14

J Pharmacol Sci 124, 123 – 128 (2014)

Journal of Pharmacological Sciences

Current Perspective

New Insights Into the Pharmacological Potential of Plant Flavonoids in the Catecholamine System

Nobuyuki Yanagihara[1], Han Zhang[2], Yumiko Toyohira[1], Keita Takahashi[1], Susumu Ueno[3], Masato Tsutsui[4], and Kojiro Takahashi[1]

[1]*Department of Pharmacology, School of Medicine,* [3]*Department of Occupational Toxicology, Institute of Industrial Ecological Sciences, University of Occupational and Environmental Health, 1-1, Iseigaoka, Yahatanishi-ku, Kitakyushu 807-8555, Japan*
[2]*Research Center of Traditional Chinese Medicine, Tianjin University of Traditional Chinese Medicine, 88 Yuquan Road, Nankai District, Tianjin 300193, China*
[4]*Department of Pharmacology, Graduate School of Medicine, University of The Ryukyus, Okinawa 903-0215, Japan*

Received November 7, 2013; Accepted December 12, 2013

Abstract. Flavonoids are biologically active polyphenolic compounds widely distributed in plants. Recent research has focused on high dietary intake of flavonoids because of their potential to reduce the risks of diseases such as cardiovascular diseases, diabetes, and cancers. We report here the effects of plant flavonoids on catecholamine signaling in cultured bovine adrenal medullary cells used as a model of central and peripheral sympathetic neurons. Daidzein (0.01 – 1.0 μM), a soy isoflavone, stimulated ^{14}C-catecholamine synthesis through plasma membrane estrogen receptors. Nobiletin (1.0 – 100 μM), a citrus polymethoxy flavone, enhanced ^{14}C-catecholamine synthesis through the phosphorylation of Ser19 and Ser40 of tyrosine hydroxylase, which was associated with $^{45}Ca^{2+}$ influx and catecholamine secretion. Treatment with genistein (0.01 – 10 μM), another isoflavone, but not daidzein, enhanced [^{3}H]noradrenaline uptake by SK-N-SH cells, a human noradrenergic neuroblastoma cell line. Daidzein as well as nobiletin ($\geq$ 1.0 μM) inhibited catecholamine synthesis and secretion induced by acetylcholine, a physiological secretagogue. The present review shows that plant flavonoids have various pharmacological potentials on the catecholamine system in adrenal medullary cells, and probably also in sympathetic neurons.

Keywords: adrenal medulla, catecholamine, flavonoid, membrane estrogen receptor, tyrosine hydroxylase

Introduction

Flavonoids are a group of plant secondary metabolites with variable phenolic structures and are found in plants fruits, vegetables, roots, stems, flowers, wine, tea, and traditional Chinese herbs (1, 2). More than 5,000 individual flavonoids have been identified, which are classified into at least 10 subgroups according to their chemical structure (3). In these flavonoids, 6 principal subgroups (flavones, flavonols, flavanones, flavanols, isoflavones, and anthocyanidins) are relatively common in human diets (Fig. 1) (4). The different flavonoids have diverse biological functions, including protection against ultraviolet radiation and phytopathogens, auxin transport, the coloration of flowers, and visual signals (1, 3). Furthermore, recent research has focused on high dietary intake of plant flavonoids because flavonoids may have potential pharmacological benefits associated with reduced risks of age and life style–related diseases such as cardiovascular diseases, diabetes, and cancers (4).

Adrenal medullary cells derived from embryonic neural crests are functionally homologous to sympathetic ganglionic neurons. Our previous studies, using cultured bovine adrenal medullary cells, demonstrated that acetylcholine (ACh)-induced $^{22}Na^+$ influx via nicotinic

*Corresponding author. yanagin@med.uoeh-u.ac.jp
Published online in J-STAGE on January 31, 2014
doi: 10.1254/jphs.13R17CP

Invited article

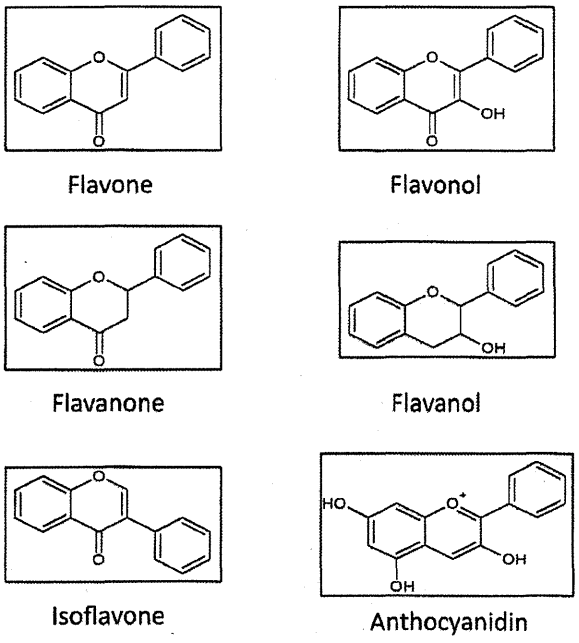

Fig. 1. Chemical structures of the main class of diet flavonoids.

acetylcholine receptor (nAChR)-ion channels increases $^{45}Ca^{2+}$ influx via voltage-dependent Ca^{2+} channels and that the enhanced Ca^{2+} influx is a prerequisite for the secretion of catecholamines (5). Furthermore, stimulation of catecholamine synthesis induced by ACh is associated with the $^{45}Ca^{2+}$ influx and the activation of tyrosine hydroxylase (6). Tyrosine hydroxylase is acutely regulated by its phosphorylation at Ser19, Ser31, and Ser40 via the activation of protein kinases, including Ca^{2+}/calmodulin-dependent protein kinase II (CaM kinase II), extracellular signal-regulated protein kinase (ERK), and cAMP-dependent protein kinase (protein kinase A), respectively (7). Catecholamine secretion mediated by stimulation of these ion channels, and the mechanism underlying the stimulation of catecholamine synthesis in adrenal medullary cells, are both thought to be similar to those of noradrenaline in sympathetic neurons and brain noradrenergic neurons. Thus, adrenal medullary cells have provided a good model for the detailed analysis of cardiovascular (6) and analgesic (8) drugs that act on catecholamine synthesis, secretion, and reuptake.

In our previous studies, treatment of bovine adrenal medullary cells with environmental estrogenic pollutants such as *p*-nonylphenol and bisphenol A stimulated catecholamine synthesis and tyrosine hydroxylase activity, probably through plasma membrane estrogen receptors (9). We further demonstrated the occurrence and functional roles of unique estrogen receptors in the plasma membranes isolated from bovine adrenal medullary cells (10). Daidzein, a flavonoid, stimulated catecholamine synthesis via the activation of extracellular signal-regulated protein kinases (ERKs) through the plasma membrane estrogen receptors (11). In the present review, we discuss our recent studies of plant flavonoids on catecholamine synthesis, secretion, and uptake in bovine adrenal medullary cells.

Regulation of catecholamine synthesis, secretion, and uptake by soy isoflavones, daidzein, and genistein

Natural estrogens induce a wide array of biological effects on cell differentiation and proliferation, homeostasis, and the female reproductive system through classical nuclear estrogen receptors (ERs), including ER-α and ER-β (12). In addition to these established mechanisms of action, a growing body of evidence suggests that estrogens have non-genomic actions via the activation of estrogen receptors in the plasma membrane. Incubation of the cells with 17β-estradiol (E_2) and daidzein for 20 min resulted in a small (15% – 25%) but significant increase in ^{14}C-catecholamine synthesis from [^{14}C]tyrosine in a concentration-dependent manner (Fig. 2A) (10, 11). Significant ($P < 0.01$) increases in ^{14}C-catecholamine synthesis induced by E_2 and daidzein were observed at 0.3 and 10 nM, respectively, and the maximum effect occurred at approximately 10 – 100 nM and 100 – 1000 nM, respectively. Tyrosine hydroxylase was also activated after incubation with E_2 or membrane-impermeable E_2–bovine serum albumin at 100 nM and daidzein as well as daidzein plus ICI182,780, an inhibitor of nuclear estrogen receptors. These findings suggest that E_2 and daidzein each activates tyrosine hydroxylase activity and then stimulates catecholamine synthesis, likely via plasma membrane estrogen receptors distinct from the more extensively investigated classical cytoplasmic/nuclear receptors.

We examined the specific binding of [^3H]E_2 to plasma membranes isolated from bovine adrenal medulla. When the plasma membranes were incubated with increasing concentrations (0.25 – 300 nM) of [^3H]E_2, specific binding was observed (10). Scatchard analysis revealed the presence of at least two classes of [^3H]E_2 binding sites. The specific binding of [^3H]E_2 (5 nM) was most strongly inhibited by E_2 and to a lesser extent by daidzein and other steroid hormones such as testosterone, corticosterone, and 17α-estradiol, the natural stereoisomer of E_2. When plasma membranes isolated from the adrenal medulla were incubated with various concentrations of daidzein and [^3H]E_2 (5 nM), the specific binding of [^3H]E_2 was competitively inhibited by daidzein in a concentration-dependent manner (10 – 1000 nM) (Fig. 2B) (11). These findings suggest that E_2 and daid-

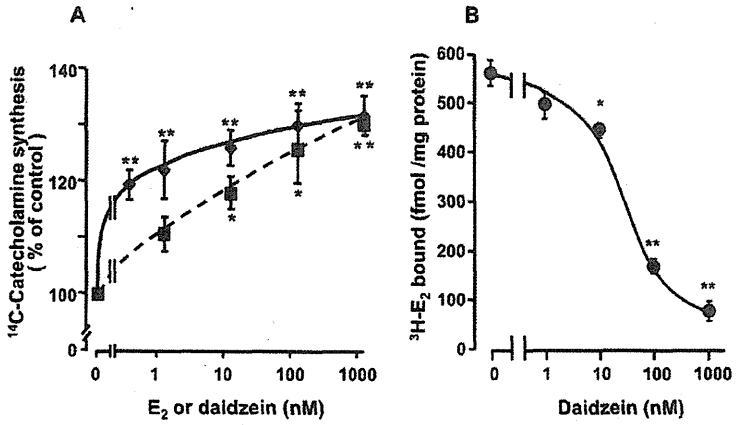

Fig. 2. Concentration–response curves of E_2 and daidzein for ^{14}C-catecholamine synthesis from [^{14}C]tyrosine (A) and concentration–inhibition curve of daidzein for [^{3}H]E_2 specific binding (B). A) Cultured cells (4 × 10^6/dish) were incubated with E_2 (closed diamonds) and daidzein (closed squares) at the indicated concentrations for 20 min at 37°C in 1.0 ml KRP buffer containing L-[U-^{14}C]tyrosine (20 μM, 1 μCi). The ^{14}C-labeled catecholamines formed are shown as the total ^{14}C-catecholamines (adrenaline, noradrenaline, and dopamine). Data are expressed as % of the control. B) Plasma membranes isolated form bovine adrenal medulla were incubated at 4°C for 30 min with various concentrations of daidzein in the presence of [^{3}H]E_2 (5 nM, 0.1 μCi). Non-specific binding was determined in the presence 1 μM of E_2 and specific binding was obtained by subtracting non-specific binding from total binding. Values shown are expressed as the mean ± S.E.M. of 4 experiments carried out in duplicate. $^{*}P < 0.05$ and $^{**}P < 0.01$, compared with the control. Data modified from Yanagihara et al. (10) and Liu et al. (11).

zein act on the same site of membrane estrogen receptors.

Recently, several types of estrogen receptor have been reported in plasma membranes, including classical nuclear estrogen receptors such as ER-α (13) as well as ER-X, a novel member of the estrogen receptor family (14), and GPR30, which has high homology with the G protein–coupled receptor superfamily in breast cancers (15). To determine whether the membrane estrogen receptors we observed are identical to, or distinct from, previously reported plasma membrane estrogen receptors, it will be necessary to precisely identify the plasma membrane estrogen receptors in future studies.

Genistein, another isoflavone, is also a major natural phytoestrogen found in soybeans. Treatment with genistein, but not daidzein, at 0.01 – 10 μM for 20 min stimulated [^{3}H]noradrenaline uptake by SK-N-SH cells, the human noradrenergic neuroblastoma cell line expressing noradrenaline transporter (16). Genistein is well-known to be a broad-spectrum inhibitor of protein tyrosine kinases, whereas daidzein is a structural analogue of genistein that lacks activity towards tyrosine kinase and is often used as a negative control of genistein in this respect (17). Since tyrophostin 25, an inhibitor of receptor-type protein tyrosine kinases, also enhanced uptake of [^{3}H]noradrenaline by cells, it seems that genistein stimulates noradrenaline transporter activity probably via the inhibition of receptor-type tyrosine kinases but not by the activation of plasma membrane estrogen receptors in the cells.

Stimulatory effects of nobiletin, a citrus flavonoid, on catecholamine synthesis and secretion

Nobiletin is a major component of polymethoxylated flavones found in the peels of citrus fruits and is used in a traditional Chinese herbal medicine. Nobiletin has attracted great interest by virtue of its broad spectrum of pharmacological activities, including antitumor, anti-oxidative, and anti-inflammatory properties (18). Furthermore, several lines of evidence have shown that nobiletin has beneficial cardiovascular effects, as well as neurotrophic and anti-dementia effects (19). In our previous study, nobiletin (1.0 – 100 μM) induced $^{45}Ca^{2+}$ influx and catecholamine secretion without $^{22}Na^{+}$ influx via the activation of voltage-dependent Ca^{2+} channels or Na^{+}/Ca^{2+} exchangers (20). Furthermore, nobiletin also simulated ^{14}C-catecholamine synthesis from [^{14}C]tyrosine and tyrosine hydroxylase activity in a concentration-dependent manner, similar to the case with $^{45}Ca^{2+}$ influx and catecholamine secretion (21).

The stimulatory effects of nobiletin on catecholamine synthesis and tyrosine hydroxylase activity were suppressed by H-89 and KN-93, inhibitors of protein kinase A and CaM kinase II, respectively, which are considered to phosphorylate tyrosine hydroxylase at Ser40 and Ser19, respectively. Indeed, nobiletin enhanced the phosphorylation of tyrosine hydroxylase at the same sites. Based on these findings, it is likely that nobiletin enhances the activity of tyrosine hydroxylase via the activation of CaM kinase II and protein kinase A,

which in turn, stimulates catecholamine synthesis in the cells. A previous report (22) showed that 4'-demethylnobiletin, a major metabolite of nobiletin in the urine of mice enhances cyclic AMP response element–mediated transcription by activating a protein kinase A/ERK pathway in cultured hippocampal neurons of mice. Therefore, it is interesting to examine the effect of its metabolites on the catecholamine synthesis.

Inhibitory effects of flavonoids on catecholamine secretion and synthesis induced by ACh, a natural secretagogue

We previously reported that ACh activates nAChR-ion channels, and this activation in turn induces Na^+ influx and subsequent Ca^{2+} influx and catecholamine secretion. K^+ (56 mM), an activator of voltage-dependent Ca^{2+} channels, directly gates voltage-dependent Ca^{2+} channels to increase Ca^{2+} influx and catecholamine secretion (5). In the present study, daidzein (1.0 – 100 μM and 100 μM) and nobiletin (0.1 – 100 μM and 1.0 – 100 μM) were found to inhibit catecholamine secretion induced by ACh (0.3 mM) and 56 mM K^+, respectively, although daidzein by itself did not affect basal catecholamine secretion and Ca^{2+} influx. These results suggest that both flavonoids attenuate catecholamine secretion induced by ACh and 56 mM K^+ through the inhibition of nAChR-ion channels and voltage-dependent Ca^{2+} channels.

To investigate the mechanism by which flavonoids inhibit ACh-induced catecholamine secretion, we examined whether or not the inhibitory effect of nobiletin on catecholamine secretion is overcome when the concentration of ACh is increased. However, they did not overcome the inhibitory effect of nobiletin and the double-reciprocal plot analysis showed a non-competitive type of inhibition. A previous review proposed that at high concentrations ($\geq$ 10 μM), steroid hormones such as estrogens could be inserted into the bilayers of cellular membranes and that direct steroid-membrane interactions alter physicochemical membrane properties, such as the fluidity and microenvironment of membrane receptors and/or ion channels, in addition to specific receptor-mediated effects (23). It is possible that daidzein and nobiletin at high concentrations may interact with these ion channels via the alteration of the membrane properties of adrenal medullary cells. However, it remains to be clarified whether or not these flavonoids may exert their effects on catecholamine secretion merely by nonspecific effects on the membrane properties.

Pharmacological significance of flavonoids' effects on the catecholamine system

The serum concentrations of daidzein have been reported to be around 200 – 350 nM in Japanese people older than 40 years (24). Furthermore, the serum concentrations of daidzein in humans consuming 3 meals per day that contained soy milk or a single soy meal can reach as high as 4.0 – 5.0 μM (25). Therefore, it seems that the concentrations used in our studies are relevant in people's daily lives because these concentrations partially overlap with those in the plasma of individuals who consume soy products.

Nobiletin is rich in the peels of citrus fruits, and the dried peels are used in a traditional Chinese herbal medicine. Nogata et al. (26) reported the contents of nobiletin in various citrus fruits: total tissue, 0.4 – 8.1 (3.93 ± 0.87) mg / 100 g; peel tissue, 1.5 – 18.5 (11.5 ± 2.2) mg / 100 g; juice vesicle tissue, 0 – 0.9 (0.25 ± 0.13) mg / 100 g. When we used 60 kg for the body weight of a man, 4.5 L of the total volume of human blood, and 0.1 of the nobiletin bioavailability (27), the calculated plasma concentrations of nobiletin might be 0.02 – 0.45 (0.22 ± 0.05) μM, 0.08 – 1.0 (0.63 ± 0.22) μM, and 0 – 0.05 (0.014 ± 0.01) μM, respectively. Indeed, the previous report (27) showed that the maximal concentrations of nobiletin in the serum and brain of mice were 0.94 mg/L (2.3 μM) and 9.27 mg/L (23 μM) or 3.6 mg/L (8.9 μM) and 22 mg/L (55 μM) after the p.o. or i.p. administration of 50 mg/kg nobiletin, respectively. Based on the previous documents, the concentrations of nobiletin (0.1 – 10 μM) used in our experiment may be appropriate, but relatively high compared to the blood concentrations of nobiletin calculated from juice vesicle tissue.

It is well documented that catecholamines play pivotal roles in the regulation of normal functions, not only in central and peripheral noradrenergic neurons as a neurotransmitter but also in adrenal medulla as an endocrine hormone. Flavonoids, including daidzein and nobiletin, by themselves induce a small but significant increase in catecholamine synthesis and/or secretion, suggesting that these flavonoids strengthen or enhance the sympatho-adrenal system.

On the other hand, several lines of evidence have shown that prolonged stress-induced over-expression of catecholamines contributes to the involvement and augmentation of cardiovascular diseases such as heart failure, atherosclerosis, coronary heart failure, and hypertension. Indeed, chronic heart failure is associated with the activation of the sympathetic nervous system as manifested by increased circulating catecholamines and increased regional activity of the sympathetic nervous system (28). Chronic stress responses can be associated with disease symptoms such as peptic ulcers or cardiovascular disorders (29). Recently, Hara et al. (30) reported that the stress hormone adrenaline stimu-

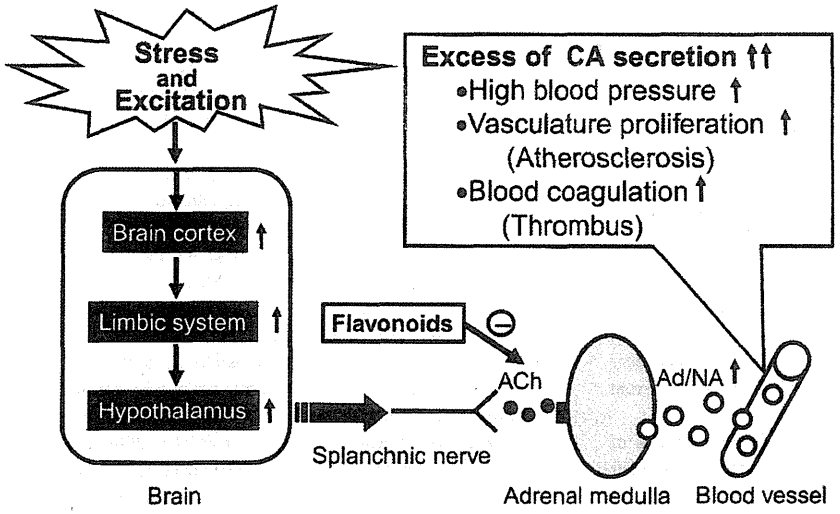

Fig. 3. Inhibitory mechanism of flavonoids on stress or excitation-induced excess of catecholamine secretion. Prolonged and strong stress or excitation stimulates the brain cortex, limbic system, and hypothalamus, which evoke acetylcholine release from the splanchnic sympathetic nerves. Released acetylcholine induces a massive secretion of adrenaline/noradrenaline from the adrenal medulla, which may cause various deleterious symptoms or diseases such as high blood pressure (hypertension), vasculature proliferation (atherosclerosis), and blood coagulation (thrombus).

Table 1. Summary of flavonoids' effects on catecholamine synthesis, secretion, and uptake

Flavonoids	CA synthesis		CA secretion		NA uptake	[^{3}H] E_2 binding
	basal	ACh	basal	ACh		
Daidzein	↑	↓	→	↓	→	↓
Genistein	N.D.	N.D.	N.D.	N.D.	↑	↓
Nobiletin	↑	↓	↑	↓	N.D.	→

CA, catecholamine; NA, noradrenaline; E_2, 17β-estradiol; ACh, ACh-stimulated; N.D., not determined; →, no effect; ↑, stimulation; ↓, inhibition.

lates β_2-adrenoceptors, which in turn induces the Gs-protein–dependent activation of protein kinase A and the β-arrestin-mediated signaling pathway, and then suppresses p53 levels and triggers DNA damage. From these previous and present results, it gives rise to the possibility that flavonoids suppress the hyperactive catecholamine system induced by prolonged stress or emotional excitation which evokes the secretion of ACh from the splanchnic nerves and stimulates a massive secretion of catecholamines from the adrenal medulla (Fig. 3).

Future perspectives

What major pending problems or questions does the present study reveal? While the in vitro effects of plant flavonoids have been well clarified using cultured bovine adrenal medullary cells or SK-N-SH cells, the in vivo effects are not as clear. Therefore, to confirm the effects of these flavonoids on the catecholamine system, further in vivo studies on the effects of the administration of daidzein, genistein, and nobiletin to animals or humans will be needed in the near future. Furthermore, the question arises as to how best to demonstrate the protective effects of flavonoids on stress-induced catecholamine synthesis and secretion. The protective effects of flavonoids against stress should be examined using laboratory animals under various stress conditions. Analysis with in vivo studies will provide more conclusive information and add to our knowledge about the pharmacological actions of plant flavonoids on the catecholamine system.

Concluding remarks

Flavonoids are major natural products in plants. In the present review, we have demonstrated that plant flavonoids such as daidzein, genistein, and nobiletin exert a variety of effects on catecholamine signaling, including catecholamine synthesis, secretion, and uptake in the adrenal medulla (Table 1). These findings may provide new insight into the pharmacological potentials of plant flavonoids on the catecholamine system.

Acknowledgments

This research was supported, in part, by Grants-in-Aid (23617035, 23590159, 23617036, and 24890286) for Scientific Research (C) from the Japan Society for the Promotion of Science.

Conflicts of Interest

The authors have no conflicts of interest to report.

References

1 Nijveldt RJ, van Nood E, van Hoorn DE, Boelens PG, van Norren K, van Leeuwen PA. Flavonoids: a review of probable mechanisms of action and potential applications. Am J Clin Nutr. 2001;74:418–425.

2 Ren ZL, Zuo PP. Neural regeneration: role of traditional Chinese medicine in neurological diseases treatment. J Pharmacol Sci. 2012;120:139–145.

3 Falcone Ferreyra ML, Rius SP, Casati P. Flavonoids: biosynthesis, biological functions, and biotechnological applications. Front Plant Sci. 2012;3:222.

4 Lu MF, Xiao ZT, Zhang HY. Where do health benefits of flavonoids come from? Insights from flavonoid targets and their evolutionary history. Biochem Biophys Res Commun. 2013;434: 701–704.

5 Wada A, Takara H, Izumi F, Kobayashi H, Yanagihara N. Influx of ^{22}Na through acetylcholine receptor-associated Na channels: relationship between ^{22}Na influx, ^{45}Ca influx and secretion of catecholamines in cultured bovine adrenal medulla cells. Neuroscience. 1985;15:283–292.

6 Yanagihara N, Wada A, Izumi F. Effects of α_2-adrenergic agonists on carbachol-stimulated catecholamine synthesis in cultured bovine adrenal medullary cells. Biochem Pharmacol. 1987;36: 3823–3828.

7 Dunkley PR, Bobrovskaya L, Graham ME, von Nagy-Felsobuki EI, Dickson PW. Tyrosine hydroxylase phosphorylation: regulation and consequences. J Neurochem. 2004;91:1025–1043.

8 Obara G, Toyohira Y, Inagaki H, Takahashi K, Horishita T, Kawasaki T, et al. Pentazocine inhibits norepinephrine transporter function by reducing its surface expression in bovine adrenal medullary cells. J Pharmacol Sci. 2013;121:138–147.

9 Yanagihara N, Toyohira Y, Ueno S, Tsutsui M, Utsunomiya K, Liu M, et al. Stimulation of catecholamine synthesis by environmental estrogenic pollutants. Endocrinology. 2005;146:265–272.

10 Yanagihara N, Liu M, Toyohira Y, Tsutsui M, Ueno S, Shinohara Y, et al. Stimulation of catecholamine synthesis through unique estrogen receptors in the bovine adrenomedullary plasma membrane by 17β-estradiol. Biochem Biophys Res Commun. 2006; 339:548–553.

11 Liu M, Yanagihara N, Toyohira Y, Tsutsui M, Ueno S, Shinohara Y. Dual effects of daidzein, a soy isoflavone, on catecholamine synthesis and secretion in cultured bovine adrenal medullary cells. Endocrinology. 2007;148:5348–5354.

12 Beato M, Herrlich P, Schutz G. Steroid hormone receptors: many actors in search of a plot. Cell. 1995;83:851–857.

13 Norfleet AM, Clarke CH, Gametchu B, Watson CS. Antibodies to the estrogen receptor-α modulate rapid prolactin release from rat pituitary tumor cells through plasma membrane estrogen receptors. FASEB J. 2000;14:157–165.

14 Toran-Allerand CD, Guan X, MacLusky NJ, Horvath TL, Diano S, Singh M, et al. ER-X: a novel, plasma membrane-associated, putative estrogen receptor that is regulated during development and after ischemic brain injury. J Neurosci. 2002;22:8391–8401.

15 Carmeci C, Thompson DA, Ring HZ, Francke U, Weigel RJ. Identification of a gene (GPR30) with homology to the G-protein-coupled receptor superfamily associated with estrogen receptor expression in breast cancer. Genomics. 1997;45:607–617.

16 Toyohira Y, Ueno S, Tsutsui M, Itoh H, Sakai N, Saito N, et al. Stimulatory effects of the soy phytoestrogen genistein on noradrenaline transporter and serotonin transporter activity. Mol Nutr Food Res. 2010;54:516–524.

17 Akiyama T, Ishida J, Nakagawa S, Ogawara H, Watanabe S, Itoh N, et al. Genistein, a specific inhibitor of tyrosine-specific protein kinases. J Biol Chem. 1987;262:5592–5595.

18 Murakami A, Nakamura Y, Torikai K, Tanaka T, Koshiba T, Koshimizu K, et al. Inhibitory effect of citrus nobiletin on phorbol ester-induced skin inflammation, oxidative stress, and tumor promotion in mice. Cancer Res. 2000;60:5059–5066.

19 Onozuka H, Nakajima A, Matsuzaki K, Shin RW, Ogino K, Saigusa D, et al. Nobiletin, a citrus flavonoid, improves memory impairment and Abeta pathology in a transgenic mouse model of Alzheimer's disease. J Pharmacol Exp Ther. 2008;326:739–744.

20 Zhang H, Toyohira Y, Ueno S, Shinohara Y, Itoh H, Furuno Y, et al. Dual effects of nobiletin, a citrus polymethoxy flavone, on catecholamine secretion in cultured bovine adrenal medullary cells. J Neurochem. 2010;114:1030–1038.

21 Zhang H, Yanagihara N, Toyohira Y, Takahashi K, Inagaki H, Satoh N, et al. Stimulatory effect of nobiletin, a citrus polymethoxy flavone, on catecholamine synthesis through Ser^{19} and Ser^{40} phosphorylation of tyrosine hydroxylase in cultured bovine adrenal medullary cells. Naunyn-Schmiedeberg's Arch Pharmacol. 2014;387:15–22.

22 Al Rahim M, Nakajima A, Saigusa D, Tetsu N, Maruyama Y, Shibuya M, et al. 4'-Demethylnobiletin, a bioactive metabolite of nobiletin enhancing PKA/ERK/CREB signaling, rescues learning impairment associated with NMDA receptor antagonism via stimulation of the ERK cascade. Biochemistry. 2009;48: 7713–7721.

23 Falkenstein E, Tillmann HC, Christ M, Feuring M, Wehling M. Multiple actions of steroid hormones--a focus on rapid, nongenomic effects. Pharmacol Rev. 2000;52:513–556.

24 Morton MS, Arisaka O, Miyake N, Morgan LD, Evans BA. Phytoestrogen concentrations in serum from Japanese men and women over forty years of age. J Nutr. 2002;132:3168–3171.

25 King RA, Bursill DB. Plasma and urinary kinetics of the isoflavones daidzein and genistein after a single soy meal in humans. Am J Clin Nutr. 1998;67:867–872.

26 Nogata Y, Sakamoto K, Shiratsuchi H, Ishii T, Yano M, Ohta H. Flavonoid composition of fruit tissues of citrus species. Biosci Biotechnol Biochem. 2006;70:178–192.

27 Saigusa D, Shibuya M, Jinno D, Yamakoshi H, Iwabuchi Y, Yokosuka A, et al. High-performance liquid chromatography with photodiode array detection for determination of nobiletin content in the brain and serum of mice administrated the natural compound. Anal Bioanal Chem. 2011;400:3635–3641.

28 Freedman NJ, Lefkowitz RJ. Anti-β_1-adrenergic receptor antibodies and heart failure: causation, not just correlation. J Clin Invest. 2004;113:1379–1382.

29 Goldstein DS. Catecholamines and stress. Endocr Regul. 2003; 37:69–80.

30 Hara MR, Kovacs JJ, Whalen EJ, Rajagopal S, Strachan RT, Grant W, et al. A stress response pathway regulates DNA damage through β_2-adrenoreceptors and β-arrestin-1. Nature. 2011;477: 349–353.

J Pharmacol Sci 124, 66 – 75 (2014)

Journal of Pharmacological Sciences

Full Paper

Effects of Selective Estrogen Receptor Modulators on Plasma Membrane Estrogen Receptors and Catecholamine Synthesis and Secretion in Cultured Bovine Adrenal Medullary Cells

Hirohide Inagaki[1,4], Yumiko Toyohira[1], Keita Takahashi[1], Susumu Ueno[2], Go Obara[3], Toshinori Kawagoe[4], Masato Tsutsui[5], Toru Hachisuga[4], and Nobuyuki Yanagihara[1,*]

[1]*Department of Pharmacology, School of Medicine,* [2]*Department of Occupational Toxicology, Institute of Industrial Ecological Sciences,* [3]*Department of Anesthesiology, School of Medicine,* [4]*Department of Obstetrics and Gynecology, School of Medicine, University of Occupational and Environmental Health, 1-1, Iseigaoka, Yahatanishi-ku, Kitakyushu 807-8555, Japan*

[5]*Department of Pharmacology, Graduate School of Medicine, University of The Ryukyus, Okinawa 903-0215, Japan*

Received August 28, 2013; Accepted November 7, 2013

Abstract. We previously reported the occurrence and function of plasma membrane estrogen receptors in cultured bovine adrenal medullary cells. Here we report the effects of raloxifene and tamoxifen, selective estrogen receptor modulators, on plasma membrane estrogen receptors and catecholamine synthesis and secretion in these cells. Raloxifene caused dual effects on the specific binding of [^{3}H]17β-estradiol to the plasma membranes isolated from bovine adrenal medulla; that is, it had a stimulatory effect at 1.0 – 10 nM but an inhibitory effect at 1.0 – 10 μM, whereas tamoxifen (1.0 nM – 10 μM) increased binding at all concentrations (except for 100 nM). Tamoxifen at 100 nM caused a significant increase in basal ^{14}C-catecholamine synthesis from [^{14}C]tyrosine, whereas tamoxifen and raloxifene at higher concentrations attenuated basal and acetylcholine-induced ^{14}C-catecholamine synthesis. Raloxifene (0.3, 1.0, and 3 – 100 μM) and tamoxifen (10 – 100 μM) also suppressed catecholamine secretion and $^{45}Ca^{2+}$ and $^{22}Na^{+}$ influx, respectively, induced by acetylcholine. Raloxifene (1.0 μM) inhibited Na^{+} current evoked by acetylcholine in *Xenopus* oocytes expressing $\alpha4\beta2$ neuronal nicotinic acetylcholine receptors. The present findings suggest that raloxifene and tamoxifen at low concentrations allosterically modulate plasma membrane estrogen receptors and at high concentrations inhibit acetylcholine-induced catecholamine synthesis and secretion by inhibiting Na^{+} and Ca^{2+} influx in bovine adrenal medulla.

Keywords: adrenal medulla, catecholamine synthesis and secretion, plasma membrane estrogen receptor, raloxifene, selective estrogen receptor modulator

Introduction

Selective estrogen receptor modulators (SERMs) are compounds that bind to nuclear or classical estrogen receptors (ERs) and exert either estrogenic or anti-estrogenic effects depending on the specific organs (1, 2). At present, at least two SERMs, tamoxifen for the treatment and prevention of breast cancer and raloxifene for the prevention of osteoporosis, are clinically available in Japan (3). Although the precise molecular mechanisms by which SERMs exert their clinical effects are unknown, their estrogenic or anti-estrogenic actions at target tissues are mediated through two ERs, ERα, and ERβ (4). In addition to the genomic ER actions, several lines of evidence have shown that SERMs acutely modulate ionic current through neuronal nicotinic acetylcholine receptors (nAChRs)-ion channels (5, 6) and also modulate functions of the cardiovascular systems (3). Furthermore, estrogens and raloxifene are reported to inhibit catecholamine secretion from rat and bovine

*Corresponding author. yanagin@med.uoeh-u.ac.jp
Published online in J-STAGE on December 27, 2013
doi: 10.1254/jphs.13155FP

adrenal medullary cells (7) and PC12 cells (8). These results suggest that SERMs directly affect ion channels and subsequent cellular functions in a non-genomic manner.

Adrenal medullary cells are derived from the embryonic neural crest and share many physiological and pharmacological properties with postganglionic sympathetic neurons. Stimulation of AChRs in the cells increases the synthesis of catecholamines and causes the secretion of catecholamines into the systemic circulation (9, 10). In bovine adrenal medullary cells, at least three distinct types of ionic channels are involved in catecholamine secretion (11): nAChR-ion channels, voltage-dependent Na^+ channels, and voltage-dependent Ca^{2+} channels. In these cells, previous studies have shown that either carbachol (a synthetic derivative of ACh)-induced Na^+ influx via nAChR-ion channels or veratridine-induced Na^+ influx via voltage-dependent Na^+ channels increases Ca^{2+} influx via voltage-dependent Ca^{2+} channels, a prerequisite for the secretion (7, 11) and synthesis (10) of catecholamines. In contrast, high K^+ directly gates voltage-dependent Ca^{2+} channels to increase Ca^{2+} influx without increasing Na^+ influx (11).

Previously, we reported the occurrence and pharmacological characterization of estrogen receptors in the plasma membrane of bovine adrenal medulla (12). Furthermore, phytoestrogens such as daidzein (13) and resveratrol (14) increased catecholamine synthesis through the plasma membrane estrogen receptors. In the present study, we examined the effects of two SERMs, raloxifene and tamoxifen, on [^{3}H]17β-estradiol (17β-E_2) binding to the membrane estrogen receptors, as well as catecholamine synthesis and secretion in cultured bovine adrenal medullary cells. We found that SERMs allosterically modulate [^{3}H]17β-E_2 binding to plasma membrane estrogen receptors and positively or negatively influence catecholamine synthesis and secretion in the cells.

Materials and Methods

Materials

Oxygenated Krebs-Ringer phosphate (KRP) buffer was used throughout. Its composition is as follows: 154 mM NaCl, 5.6 mM KCl, 1.1 mM $MgSO_4$, 2.2 mM $CaCl_2$, 0.85 mM NaH_2PO_4, 2.15 mM Na_2HPO_4, and 10 mM glucose, adjusted pH to 7.4. Reagents were obtained from the following sources: Eagle's minimum essential medium (MEM) (Nissui Pharmaceutical, Tokyo); calf serum (Cell Culture Technologies, Zürich, Switzerland); collagenase (Nitta Zerachin, Osaka); raloxifene, tamoxifen, 17β-E_2, ACh, veratridine (Sigma Chemical Co., St. Louis, MO, USA); [2,4,6,7-^{3}H]17β-E_2 (3515 GBq/mmol), [^{22}Na]Cl, [^{45}Ca]Cl_2, and L-[U-^{14}C]tyrosine (Perkin-Elmer, Ltd., Boston, MA, USA). Raloxifene and tamoxifen were dissolved in 100% dimethyl sulfoxide and then diluted in a reaction medium before use at a final concentration of dimethyl sulfoxide not exceeding 0.5% unless otherwise specified.

Isolation and primary culture of bovine adrenal medullary cells

Bovine adrenal medullary cells were isolated by collagenase digestion of adrenal medullary slices according to the previously reported method (15, 16). Cells were suspended in Eagle's MEM containing 10% calf serum, 3 μM cytosine arabinoside, and several antibiotics, and maintained in monolayer culture at a density of 4×10^6 cells per dish (35 mm dish; Falcon, Becton Dickinson Labware, Franklin Lakes, NJ, USA) or 10^6 cells per well (24-well plate; Corning Life Science, Lowell, MA, USA) at 37°C under a humidified atmosphere of 5% CO_2 and 95% air. The cells were used for experiments between 2 and 5 days of culture.

[^{3}H]17β-E_2 binding to plasma membranes isolated from adrenal medulla

Plasma membranes were isolated from bovine adrenal medulla as described previously (12, 13). The specific binding of [^{3}H]17β-E_2 was determined by incubating plasma membranes (30 μg protein) in Krebs-Ringer HEPES (KRH) buffer (composition: 125 mM NaCl, 4.8 mM KCl, 2.6 mM $CaCl_2$, 1.2 mM $MgSO_4$, 5.6 mM glucose, and 25 mM HEPES-Tris, pH 7.4) (final volume of 200 μL) with various concentrations (0.001 – 10 μM) of raloxifene or tamoxifen and [^{3}H]17β-E_2 (5 nM, 0.1 μCi) at 4°C for 30 min. Then [^{3}H]17β-E_2 bound to the membranes was separated from free ligand by filtration through a GF/C glass fiber filter (Whatman, Maidstone, UK), and the filter was washed 3 times with the ice-cold binding buffer. Specific binding of [^{3}H]17β-E_2 was defined as the total binding minus non-specific binding, which was determined in the presence of 17β-E_2 (1.0 μM) (12).

^{14}C-catecholamine synthesis from [^{14}C]tyrosine in the cells

After preincubation for 10 min, cells were incubated with 20 μM L-[U-^{14}C]tyrosine (1 μCi) in KRP buffer in the presence or absence of various concentrations of raloxifene or tamoxifen and 300 μM ACh at 37°C for 20 min. After removing the incubation medium by aspiration, cells were harvested in 0.4 M perchloric acid and centrifuged at $1600 \times g$ for 10 min. ^{14}C-Labelled catechol compounds were separated further by ion exchange chromatography on Duolite C-25 columns (H^+-type, 0.4 × 7.0 cm) (10) and counted for the radioac-

tivity by a Packard Tri-Carb 2900TR liquid scintillation counter. ^{14}C-Catecholamine synthesis was expressed as the sum of the ^{14}C-catecholamines (adrenaline, noradrenaline, and dopamine).

Catecholamine secretion from cultured bovine adrenal medullary cells

The secretion of catecholamines was measured as described previously (15). After preincubation with or without raloxifene or tamoxifen at 37°C for 10 min, the cells (10^6 per well) were incubated with or without the SERMs in the presence or absence of various secretagogues at 37°C for another 10 min. After the reaction, the incubation medium was transferred immediately to a test tube containing perchloric acid (final concentration, 0.4 M). Catecholamines (noradrenaline and adrenaline) secreted into the medium were adsorbed onto aluminum hydroxide and estimated by the ethylendiamine condensation method using a fluorescence spectrophotometer (F-2500; Hitachi, Tokyo) with excitation and emission wavelengths of 420 and 540 nm, respectively.

$^{22}Na^+$ and $^{45}Ca^{2+}$ influx by the cells

The influx of $^{22}Na^+$ and $^{45}Ca^{2+}$ was measured as reported previously (11). After preincubation with or without raloxifene or tamoxifen at 37°C for 10 min, the cells (4×10^6 per dish) were incubated with 1.5 μCi of ^{22}NaCl or 1.5 μCi of $^{45}CaCl_2$ at 37°C for 5 min in the presence or absence of 300 μM ACh and various concentrations of the SERMs in KRP buffer. After incubation, the cells were washed 3 times with ice-cold KRP buffer, solubilized in 10% Triton X-100, and counted for radioactivity of $^{22}Na^+$ and $^{45}Ca^{2+}$ by an Aloka ARC-2005 gamma counter and a Packard Tri-Carb 2900TR liquid scintillation counter, respectively.

Expression of nAChRs in Xenopus oocytes and electrophysiological recordings

Isolation and microinjection of *Xenopus* oocytes was performed as described previously (17, 18). In brief, the cDNA encoding the α4 and β2 subunits of rat neuronal nAChR, subcloned into pcDNAI/Neo (Invitogen, Carlsbad, CA, USA) vector, was kindly provided from Dr. James W. Patrick (Division of Neuroscience, Baylor College of Medicine, Houston, TX, USA). Oocytes were injected with cDNAs (1.5 ng/30 nL) and electrophysiological recordings were performed 2 – 3 days after injection. Each oocyte was perfused (2 mL/min) with Ba^{2+}-Ringer's solution (115 mM NaCl, 2.5 mM KCl, 1.8 mM $BaCl_2$, and 10 mM HEPES, pH 7.4) containing 1 μM atropine sulfate, to minimize the effects of secondary activated Ca^{2+}-dependant Cl^- currents and then impaled with 2 glass electrodes (1 – 5 MΩ) filled with 3 M KCl and clamped at −70 mV using the OC-725C Oocyte Clamp Amplifier (Harvard Apparatus, Inc., Holliston, MA, USA). ACh was applied for 30 s to obtain the maximum (peak) current used as a measure of drug response. We examined the effect of raloxifene (1 μM) on Na^+ current induced by ACh at a concentration that produced 50% of the maximal effect (EC_{50}) of ACh (1 mM).

Statistical analyses

All experiments were performed in duplicate or triplicate, and each experiment was repeated at least three times. All values are given as the mean ± S.E.M. The significance of differences between means was evaluated using one-way analysis of variance (ANOVA). When a significant F value was found by ANOVA, Dunnett's or Scheffe's test for multiple comparisons was used to identify differences among the groups. Values were considered statistically different when the *P*-value was less than 0.05. Statistical analyses were performed using PRISM for Windows version 5.0J software (Abacus Concept, Berkeley, CA, USA).

Results

Effects of raloxifene and tamoxifen on [^{3}H]17β-E_2 binding to plasma membranes

We first examined the effects of raloxifene and tamoxifen on the specific binding of [^{3}H]17β-E_2 to plasma membranes isolated from bovine adrenal medulla. When plasma membranes were incubated with these SERMs at various concentrations, the specific binding of [^{3}H]17β-E_2 was significantly increased by raloxifene and tamoxifen at 1.0 – 10 nM (Fig. 1A) and 1.0 nM – 10 μM (except for 100 nM) (Fig. 1B), respectively, but inhibited by raloxifene at 1.0 – 10 μM (Fig. 1A). These results suggest that the SERMs interact with plasma membrane estrogen receptors to positively or negatively modulate specific [^{3}H]17β-E_2 binding.

Effects of raloxifene and tamoxifen on basal and ACh-induced ^{14}C-catecholamine synthesis from [^{14}C]tyrosine in the cells

Bovine adrenal medullary cells were incubated with 20 μM [^{14}C]tyrosine in KRP buffer in the presence or absence of various concentrations of SERMs at 37°C for 20 min. As shown in Fig. 2B, tamoxifen at 100 nM significantly increased ^{14}C-catecholamine synthesis from [^{14}C]tyrosine, but raloxifene and tamoxifen at higher concentrations (0.1 – 1.0 and 1.0 – 10 μM, respectively) inhibited it (Fig. 2: A and B). Raloxifene (100 nM) and tamoxifen (100 nM and 1.0 μM) had little effect on [^{14}C]tyrosine uptake by the cells (data not shown),

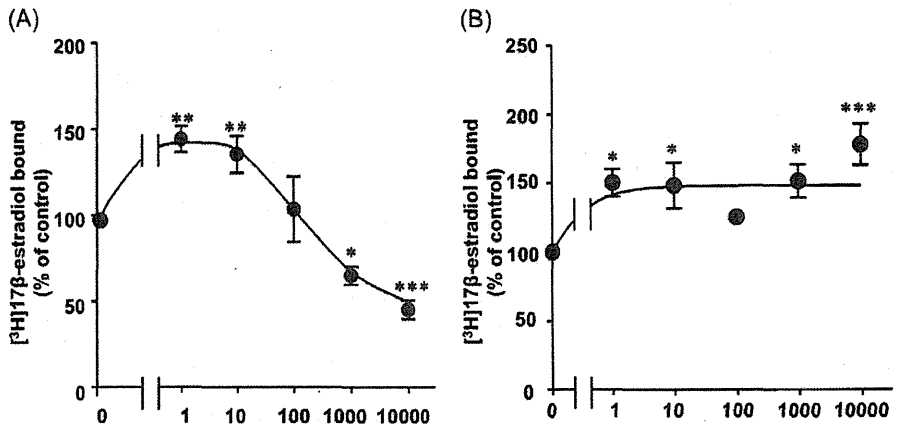

Fig. 1. Effects of raloxifene (A) and tamoxifen (B) on the specific binding of [^{3}H]17β-estradiol (17β-E_2) to plasma membranes isolated from bovine adrenal medulla. Plasma membranes (30 μg/tube) were incubated with [^{3}H]17β-E_2 (5 nM) and various concentrations of raloxifene (A) or tamoxifen (B) for 30 min at 4°C. Non-specific binding of [^{3}H]17β-E_2 was determined in the presence of 200-fold excess concentrations of 17β-E_2, and specific binding was obtained by subtracting non-specific binding from total binding. Control specific binding of [^{3}H]17β-E_2 [150 ± 15 (A) and 208 ± 36 (B) fmol/mg protein] was assigned a value of 100% and the data are expressed as % of control. Values shown are the mean ± S.E.M. of 4 experiments carried out in duplicate. $*P < 0.05$, $**P < 0.01$, and $***P < 0.001$; compared to each control.

suggesting that the SERMs do not affect tyrosine uptake by the cells. ACh (300 μM) increased ^{14}C-catecholamine synthesis, which raloxifene and tamoxifen suppressed significantly (1.0 μM and 10 – 100 μM, respectively) in a concentration-dependent manner (Fig. 2: C and D).

Effects of pretreatment with raloxifene and tamoxifen on catecholamine secretion induced by ACh in the cells

Raloxifene (1 μM) and tamoxifen (10 μM) did not significantly affect basal secretion of catecholamines (control = 2.85% ± 0.17%, raloxifene = 3.21% ± 0.41%, tamoxifen = 3.47% ± 0.23% of the total catecholamines). Stimulation of nAChR-ion channels by ACh, a physiological secretagogue, caused catecholamine secretion corresponding to 16.79% ± 0.75% of the total catecholamines in the cells (Fig. 3A). Pretreatment of cells with raloxifene (1 μM) (Fig. 3A) and tamoxifen (10 μM) (Fig. 3B) for 0, 5, 10, 20, and 30 min caused a time-dependent decrease in catecholamine secretion induced by ACh for up to 30 min, with a continuously maximal reduced level occurring at 10 min. Therefore, the effect of SERMs on catecholamine secretion was evaluated using cells pretreated with SERMs for 10 min.

We examined the effects of raloxifene (1 μM) and tamoxifen (10 μM) on catecholamine secretion induced by other secretagogues. Veratridine (100 μM), an activator of voltage-dependent Na^+ channels, or 56 mM K^+, an activator of voltage-dependent Ca^{2+} channels, caused catecholamine secretion corresponding to 24.28% ± 1.58% and 19.47% ± 1.11% of the total catecholamines, respectively (Fig. 4A). Raloxifene (1 μM) (Fig. 4A) and tamoxifen (10 μM) (Fig. 4B) had little effect on catecholamine secretion induced by veratridine and high K^+.

Concentration–inhibition curves for the effects of raloxifene or tamoxifen on ACh-induced catecholamine secretion and $^{22}Na^+$ and $^{45}Ca^{2+}$ influx

Pretreatment of cells with raloxifene (0.3, 1, 10, and 100 μM) or tamoxifen (10, 30, and 100 μM) for 10 min reduced ACh-induced secretion of catecholamines to 81.0%, 65.0%, 35.1%, and 33.0% (Fig. 5A) or to 49.0%, 43.1%, and 25.4% (Fig. 6A), respectively, of ACh alone in a concentration-dependent manner. Raloxifene suppressed ACh (300 μM)-induced $^{45}Ca^{2+}$ influx at 1.0 – 100 μM (Fig. 5B), and ACh (300 μM)-induced $^{22}Na^+$ influx at 0.3 – 100 μM (Fig. 5C). Tamoxifen also inhibited ACh-induced $^{45}Ca^{2+}$ influx (Fig. 6B) and $^{22}Na^+$ influx at 10 – 100 μM (Fig. 6C).

Inhibitory mode of raloxifene or tamoxifen on $^{22}Na^+$ influx induced by ACh

We attempted to determine whether either SERM competes with ACh for binding sites on the nAChRs. When the concentration of ACh in the incubation medium increased, the inhibition of $^{22}Na^+$ influx induced by either SERM was not overcome by increasing concentrations (10 – 300 μM) of ACh (Fig. 7: A and B), indicating that neither SERM competes with ACh for the binding sites on nAChRs.